Spin observables in the $p + n \to p + \Lambda$ reaction

by

Tatoku Ogaito

Submitted to Graduate School of Science,
in partial fulfillment of the requirements for the degree of

Doctor of Philosophy

at the

OSAKA UNIVERSITY

February, 1999

Abstract

The purpose of the present paper is to demonstrate that $p + n \to p + \Lambda$ reaction is useful to investigate the strangeness changing weak interaction between baryons(BB). It is shown that one can study the interference terms of parity-conserving and violating, isospin-singlet and triplet, and spin-triplet and singlet using polarization observables with the polarized proton beam and the polarization of Λ. Using meson-exchange model of weak BB interaction in DWBA, we show those polarization observables are indeed sensitive to the spin-flavor structure of the weak BB interaction and provide us informations, which are quite different from those obtained from the study of non-mesic decay of hypernuclei. The study of $p + n \to p + \Lambda$ reaction will open a new way to the weak BB interaction.

Contents

1 Introduction

Study of the baryon-baryon(BB) interaction is one of the fundamental problems in nuclear physics. The nucleon-nucleon(NN) interaction is discussed in terms of potential between nucleons, and has been applied to nuclear many body problems. The microscopic property of the NN potential has been investigated by the model of meson-exchange between nucleons. The longest range part of the NN potential is due to the pion-exchange mechanism, and various heavy boson exchange mechanisms have been subsequently studied[1, 2]. To understand the short distance behavior of the potential, it has been shown that the quark sub-structure of the nucleon plays important role, especially, for the short range repulsion of NN potential[3]. Those boson-exchange models and phenomenological models[4] of NN potential have been tested for the NN scattering data, nuclear matter properties, and also 'exact' calculation of the few nucleon bound system. When we turned eyes to the BB interaction with $S = -1$, our knowledge of this BB interaction is still far from 'satisfactory' because of the limited data of hyperon-nucleon(YN) scattering. Here hypernuclei, the bound state of hyperon and ordinary nuclei, provide important information on the YN interaction. As a SU(3) extension of the NN interaction, the YN two-body interaction has been investigated in the model of boson-exchange[5 - 9] and also the model with the quark degrees of freedom[10]. They are examined for the YN scattering data and binding energy of light s-shell Λ-hypernuclei. Recent three-body calculation of hypertriton also has put a severe constrain on the YN interaction, especially the s-wave YN interaction [11, 12].

Weak non-leptonic BB interaction is another interesting subject. In the weak BB interaction with $\Delta S = 0$, parity violation phenomena has been studied in the ordinary nuclei[13]. Here we can only probe parity violating part of weak NN interaction because of the strong NN interaction. The parity violation in nuclei has been observed, for example, on the asymmetry of longitudinal polarized proton and circular polarization of photon in the decay of the nuclear excited states. They are investigated in the boson-exchange model of the weak NN interaction. Apart from the two-nucleon system, one need good control of the nuclear wave function to understand the parity mixture of nuclear state using boson-exchange model. In the weak BB

interaction with $\Delta S = 1$, we have a possibility to investigate both the parity-conserving and parity-violating interaction because the strong interaction conserves strangeness. Here, again the hypernuclear physics plays important role.

Soon after the discovery of the V-particle, the possibility of the weak decay of hypernuclei was discussed[14]. Λ decays into a pion and a nucleon in the non-leptonic weak process. The life time of Λ is 2.63×10^{-10} sec. In the ground states of many hypernuclei, Λ decays via the weak interaction. Their typical life is about 1.0×10^{-10} sec. One of the decay mode of Λ-hypernuclei is 'mesic decay' accompanying a pion emission. In this process, recoil momentum of the final nucleon is around 100MeV/c, which is smaller than the typical Fermi momentum of 250MeV/c in nuclei. Therefore, this process might be suppressed by the Pauli principle in heavy hypernuclei. Another mechanism, which is possible only in multi-baryon system, is 'non-mesic decay'. Basic mechanism of non-mesic decay is $YN \to NN$. Therefore weak decay of hypernuclei provides a unique opportunity to study the strangeness-changing weak BB interaction. The relevant momentum of recoiled nucleon is around 400MeV/c, because the mass difference between Λ and nucleon is fully converted into nucleon kinetic energy. Actually observed ratio of mesic-decay to non-mesic decay rate decreases as the mass of hypernuclei increases.

Recent experimental efforts at KEK and BNL on (π^+, K^+) and (K^-, π^-) reactions provide us some hints on the mechanism of the non-mesic decay of hypernuclei[15, 16]. The non-mesic decay in nuclei can be decomposed into two parts i.e., 'proton stimulated decay' $(\Lambda + p \to p + n)$ and 'neutron stimulated decay' $(\Lambda + n \to n + n)$. Together with the total non-mesic decay rate, ratio of proton and neutron stimulated non-mesic decay rates might reveal the flavor structure of the BB interaction with $\Delta S = 1$, which in principle gives an answer to the interesting question on whether $\Delta I = 1/2$ rule observed in non-mesic decay of hyperon holds also in the BB interaction with $\Delta S = 1$. The ratio of parity-conserving and parity-non-conserving strengths of the interaction was obtained from the asymmetric angular distribution of emitted protons from polarized Λ-hypernuclei[17, 18]. To extract the information on the BB interaction with $\Delta S = 1$, one may be required to provide a great deal of the knowledge on the structure of

hypernuclei, final state interaction in addition to the dynamical model of weak BB interaction.

Against this observation, one may extract the spin and isospin structure of the weak decay phenomenologically using the non-mesic decay rate of the s-shell hypernuclei[19, 20]. In the s-shell Λ-hypernuclei, all baryons are assumed to occupy the s-state. Therefore ${}^3S_1$ or ${}^1S_0$ Λ-nucleon state decays into two nucleons. The ${}^1S_0$ state decays into iso-triplet($T = 1$) NN state, while the ${}^3S_1$ state decays into the states with both $T = 1$ and $T = 0$. If the final state interaction of the outgoing nucleon with the spectator nucleons can be neglected and also the YN wave function in various s-shell nuclei are almost the same, one can extract individual strengths of spin triplet/singlet of proton- and neutron-stimulated decays. Ideally, if we extract spin-singlet,i.e.,T=1 proton and neutron-stimulated decay rate, we can test the $\Delta I = 1/2$ rule, since those two are related with each other via the isospin geometrical factor. Unfortunately, the present accuracy of the experimental data forbids us to draw a definite conclusion on the validity of the $\Delta I = 1/2$ rule[21]. One need dynamical model to understand this process furthermore.

The dynamical model of the weak $YN \to NN$ interaction has been studied by the boson-exchange model, in a quite similar way to the model of strong BB interaction[22, 23]. The long range part of the interaction is due to the process that pion emitted by the weak decay of Λ is absorbed by the other nucleon through the strong interaction, which was proposed in '50[24]. Since the early work[25, 26], one-pion-exchange mechanism has been studied in the non-mesic decay using the nuclear matter approximation or shell-model. Short range correlation and the final state distortion of nucleon are shown to be important to decrease the total decay rate[27]. In the pion-exchange model, the total non-mesic decay rates of ${}^{12}_{\Lambda}$C and ${}^{5}_{\Lambda}$He were satisfactorily explained, but failed to explain the ratio of proton- and neutron-stimulated decay rates. In these studies the parity-conserving part of the weak interaction plays important role. Since the decay from the triplet YN state, which is T=0, is dominant, the tensor-type interaction should play important role.

It is well known the strong tensor part of OPE is reduced by the exchange of rho-meson in nucleon-nucleon potential. Also, because the momentum of the final nucleon is rather large

in the non-mesic decay, it is probable that shorter range mechanism with the exchange of the heavier bosons may become important. However, one should keep in mind that boson-exchange mechanism other than pion exchange should rely on the model of physically unobservable mesonic decay of Λ. In the rho-meson exchange, the strength is determined by the factorization model[28], pole model[29] and $SU(6)_W$ model[30 - 32]. Rho-meson exchange process reduces the tensor component as expected i.e., reduces the contribution of the T=0 strength. In addition to the π and rho-exchange mechanism, effects of K and K^* exchange processes on the A=5,12 hypernuclei[33] were studied. Unfortunately these effects could not explain the ratio of proton and neutron-stimulated decay rates. It should be mentioned that we must adopt reliable wave function with the correct two-baryon short range and tensor correlation, but not ad hoc. conventional correlation.

The magnitude of parity-violation was measured by the asymmetric distribution of proton in hypernuclear production. Proton asymmetry is given by the product of polarization of hypernuclei and the asymmetry parameterα_p of the non-mesic decay. The results of the boson-exchange model seems to be consistent with the experimental data within the error. However in order to extract α_p one need theoretical value of the polarization of hypernuclei produced by the $^{12}\mathrm{C}(\pi^+, K^+)$ reaction. Recent measurement of polarization of $^{5}_{\Lambda}\mathrm{He}$ using pionic decay mode is important for the further step on the parity violation in non-mesic decay.

Is is also noticed that there have been suggested additional mechanisms such as two-pion exchange mechanism [34], three body process[35, 36], and modification of exchanged pion in nuclear matter[37]. Importance of the short range part of the weak BB interaction motivated the study of the quark exchange mechanism[38, 39] In ref [40 - 42], possible violation of the $\Delta I = 1/2$ rule in BB interaction was suggested by treating the short range part in a similar way to the NN potential.

So far no models of weak BB interaction can explain satisfactorily both the total decay rate and the ratio of proton and neutron-stimulated decay rates. Although the understanding of the weak BB interaction has been deepened by the study of the non-mesic decay of the hypernuclei, new type of observables on the weak BB process will be very useful to identify the

possible problems in the models of weak BB interaction and clarify the structure of the weak BB interaction.

The purpose of the present paper is to study the $p + n \to \Lambda + p$ reaction, and suggest that this reaction provides us a new method to study the weak BB interaction. The great advantages of this reaction compared with the weak decay of hypernuclei, is that the polarization of proton beam is under control, and that the polarization of Λ is also measurable through its weak decay. Therefore we can study the interference between spin triplet/singlet, isospin-triplet/sninglet and parity-conserving/parity-non-conserving amplitudes through the various polarization observables. They will clarify the structure of weak BB interaction more restrictively together with the weak decay of hypernuclei. The production cross section was estimated to be around 10^{-39}cm^2 from the non-mesic decay rate[43, 44]. Although the cross section is small, this experiment was shown to be feasible[44 - 46] using the sophisticated detector system in the existing accelerator. The new coming high intensity proton machine will be a possible place to study this reaction. The $p+n \to \Lambda+p$ reaction, which was originally proposed in Ref. [44 - 46] will open a new field to study the weak BB interaction.

The total cross section of the reaction was already estimated in plane wave approximation[47, 48] and OPE-model in DWBA[49]. Only proton asymmetry have been studied in the recent preprint[50]. In the present paper we will study all the possible polarization observables of the $p + n \to \Lambda + p$ reaction, and clarify their role in the study of the weak BB interaction.

The paper is organized as follows. Formalism of the polarization observables are given in section 2 using the standard multipole expansion technique. The observables include single polarization of proton and Λ, and also possible double polarizations. They are classified into parity and time-reversal conserving and violating observables. In section 3 the weak BB interaction is constructed in the meson exchange model which was used in the non-mesic decay of hypernuclei. In order to use the meson exchange model for our inverse reaction, we assumed the CP invariance of the weak Hamiltonian. With the boson-exchange model, we study the total cross section and polarization observables from the threshold energy of Λ production to the energy above the Σ production. It will be shown in section 4 that the polarization observables

are sensitive to the mechanism of weak BB interaction and hence clarify the various aspects of the weak BB interaction. Our work is summarized in section 5.

2 Formalism of $p + n \to p + \Lambda$ Reaction

We study the $NN \to YN$ reaction through the following Hamiltonian,

$$H = H_0 + V. \tag{2.1}$$

H_0 is kinetic energy of baryons including their rest masses. V is the potential energy between baryons, which is expressed by the following matrix in baryon Fock space:

$$V = \begin{pmatrix} \langle NN|V|NN\rangle & \langle NN|V|YN\rangle \\ \langle YN|V|NN\rangle & \langle YN|V|YN\rangle \end{pmatrix}. \tag{2.2}$$

Here $V_{NN}(= \langle NN|V|NN\rangle)$ and $V_{YN}(= \langle YN|V|YN\rangle)$ are the strong interaction potentials for $S = 0$ and $S = 1$ baryon systems. $V_W(= \langle YN|V|NN\rangle)$ is the $\Delta S = 1$ weak baryon-baryon potential. In the proton-neutron scattering with charge $Q = 1$, the YN Fock space consists of Λp, $\Sigma^0 p$ and $\Sigma^+ n$. Weak interaction V_W can be treated in the first order perturbation. Then, by following the standard procedure , the T-matrix element of $NN \to YN$ reaction is written in DWBA as

$$\langle f|T|i\rangle = \langle \chi^{(-)}_{YN}(\boldsymbol{p}_f)|V_W|\chi^{(+)}_{NN}(\boldsymbol{p}_i)\rangle, \tag{2.3}$$

where $\chi^{(+)}_{NN}$ and $\chi^{(-)}_{YN}$ are scattering wave functions of the NN and YN systems with the center-of-mass momenta $\boldsymbol{p}_i$ and $\boldsymbol{p}_f$, respectively.

In this section, we derive the general cross section formula of $NN \to YN$ reaction with polarized proton beam and also polarization of hyperon, and define the polarization observables. Near the threshold energy, we can restrict the angular momentum of the final YN system to the S-wave, and we can express the observables using a few dominant matrix elements. This formula may be useful to understand the physics of polarization observables and to clarify the connection between the $p + n \to p + \Lambda$ and weak non-mesonic decay of hypernuclei.

2.1 Cross section formula

Assuming the rotational invariance, the general T-matrix of $pn \to p\Lambda$ reaction in the center of mass system can be expanded into the multipole series as follows,

$$\begin{aligned}\langle s'_p s_\Lambda; \boldsymbol{p}_f | T | s_p s_n; \boldsymbol{p}_i \rangle &= \sum_{J\ell\ell' mm' SS'} (\tfrac{1}{2} s'_p \tfrac{1}{2} s_\Lambda | S'\mu')(\ell' m' S'\mu' | JM) Y_{\ell' m'}(\hat{\boldsymbol{p}}_f) \\ &\quad \times (\tfrac{1}{2} s_p \tfrac{1}{2} s_n | S\mu)(\ell m S\mu | JM) Y^*_{\ell m}(\hat{\boldsymbol{p}}_i) \\ &\quad \times \langle [\ell' \otimes S']^M_{(J)}; p_f | T | [\ell \otimes S]^M_{(J)}; p_i \rangle. \end{aligned} \tag{2.4}$$

Here s'_p, s_Λ, s_p and s_n are baryon spins, and $\boldsymbol{p}_i, \boldsymbol{p}_f$ are the momenta of initial and final proton respectively. ℓ, S and ℓ', S' are the orbital and spin angular momenta of NN and YN systems. Since the weak interaction V_W may not conserve parity, the T-matrix element is not diagonal for the spin and orbital angular momentum.

The partial wave T-matrix element $\langle [\ell' \otimes S']^M_{(J)}; p_f | T | [\ell \otimes S]^M_{(J)}; p_i \rangle$ can be expressed by using the YN and NN distorted waves and weak potential in DWBA. For this purpose, we define the partial wave expansion of NN and YN wave functions in momentum space as follows,

$$\begin{aligned}\langle \boldsymbol{p}_i NN | \chi^{(+)}_{s_p s_n} \rangle &= \sum_{S_i \ell_i JM} (\tfrac{1}{2} s_p \tfrac{1}{2} s_n | S_i \mu_i)(\ell_i m_i S_i \mu_i | JM) Y^*_{\ell_i m_i}(\hat{\boldsymbol{p}}_i) \\ &\quad \times \sum_{\ell', S'} \mathcal{Y}^M_{(\ell' S')J}(\hat{\boldsymbol{p}}) \chi^{(+)}_{i\,J}(\ell' S', p; \ell_i S_i p_i), \end{aligned} \tag{2.5}$$

$$\begin{aligned}\langle \boldsymbol{p}_f YN | \chi^{(-)}_{s_p s_n} \rangle &= \sum_{S_f \ell_f JM} (\tfrac{1}{2} s_p \tfrac{1}{2} s_n | S_f \mu_f)(\ell_f m_f S_f \mu_f | JM) Y^*_{\ell_f m_f}(\hat{\boldsymbol{p}}_f) \\ &\quad \times \sum_{\ell', S'} \mathcal{Y}^M_{(\ell' S')J}(\hat{\boldsymbol{p}}') \chi^{(-)}_{f\,J}(\ell' S', p'; \ell_f S_f p_f), \end{aligned} \tag{2.6}$$

where $\mathcal{Y}^M_{(\ell S)J}(\hat{\boldsymbol{p}})$ is defined as

$$\mathcal{Y}^M_{(\ell S)J}(\hat{\boldsymbol{p}}) = \left[Y_\ell(\hat{\boldsymbol{p}}) \otimes \left[\chi_{\frac{1}{2}} \otimes \chi_{\frac{1}{2}} \right]_{(S)} \right]^M_{(J)}. \tag{2.7}$$

It is noticed that $\boldsymbol{p}, \boldsymbol{p}'$ ($\boldsymbol{p}_i, \boldsymbol{p}_f$) are off-shell (on-shell) momenta of NN and YN systems. For YN wave function, in addition to the spin and orbital angular momentum, we have to specify the component of baryon Fock space. In a similar way, the weak transition potential V_W is also

expanded into the partial wave series as

$$\begin{aligned}
&\langle s'_p s_\Lambda; \boldsymbol{p}'|V_W|s_p s_n; \boldsymbol{p}\rangle \\
&= \sum_{J\ell\ell' mm' SS'} (\tfrac{1}{2} s'_p \tfrac{1}{2} s_\Lambda|S'\mu')(\ell' m' S'\mu'|JM) Y_{\ell' m'}(\hat{\boldsymbol{p}}') \\
&\quad \times (\tfrac{1}{2} s_p \tfrac{1}{2} s_n|S\mu)(\ell m S\mu|JM) Y^*_{\ell m}(\hat{\boldsymbol{p}})\ V_{W\,J}^{\ell' S'\,\ell S}(p', p). \qquad (2.8)
\end{aligned}$$

Using equations (2.5), (2.6), (2.8) and (2.4), we obtain the T-matrix element in terms of the radial integral in the momentum space:

$$\begin{aligned}
&\langle [\ell_f \otimes S_f]^M_{(J)}; p_f|T_J(p_f, p_i)|[\ell_i \otimes S_i]^M_{(J)}; p_i\rangle \\
&= -(2\pi)^3 \sum_{\text{'s}} \int dp'_f dp'_i {p'_f}^2 {p'_i}^2 \chi^{(-)*}_{f\,J}(\ell'_f S'_f p'_f; \ell_f S_f p_f) V_{W\,J}^{\ell'_f S'_f\ \ell'_i S'_i}(p'_f, p'_i) \chi^{(+)}_{i\,J}(\ell'_i S'_i p'_i; \ell_i S_i p_i). \qquad (2.9)
\end{aligned}$$

Here we study all possible observables with polarized proton beam and also Λ polarization. The polarization observables are easily calculated by introducing the following density matrix as

$$\rho_i \equiv \frac{1 + \boldsymbol{\sigma}_i \cdot \boldsymbol{P}_i}{2}, \qquad (2.10)$$

where i stands for proton(p) or $\Lambda(\Lambda)$ and $\boldsymbol{P}_i$ is polarization vector of particle i. Then the differential cross section is simply given by the trace calculation as

$$\frac{d\sigma}{d\Omega}(E, \boldsymbol{P}_p, \boldsymbol{P}_\Lambda) \quad = \quad NW, \qquad (2.11)$$

where W is given by the following trace of density matrix as

$$W = \mathrm{Tr}(\rho_\Lambda \hat{T} \rho_p \hat{T}^\dagger). \qquad (2.12)$$

Here $\hat{T}$ should be regarded as the spin matrix of baryons (s_p, s'_p, s_n, s_Λ). N is the phase space factor given as

$$N \quad \equiv \quad (2\pi)^4 \frac{|\boldsymbol{p}_f|}{|\boldsymbol{p}_i|} \frac{E'_p E_\Lambda E_p E_n}{E^2}, \qquad (2.13)$$

where E_i is the energy of particle i, and E is center-of-mass energy. The trace calculation could be done as follows,

$$W \ = \ \sum_{\substack{s_p \bar{s}_p s_n \\ s_\Lambda \bar{s}_\Lambda s'_p}} \langle s'_p s_\Lambda; \boldsymbol{p}'|T|s_p s_n; \boldsymbol{p}\rangle \langle s_p| \frac{1 + \boldsymbol{\sigma}_p \cdot \boldsymbol{P}_p}{2} |\bar{s}_p\rangle \langle \bar{s}_p s_n; \boldsymbol{p}|T^\dagger|s'_p \bar{s}_\Lambda; \boldsymbol{p}'\rangle \langle \bar{s}_\Lambda| \frac{1 + \boldsymbol{\sigma}_\Lambda \cdot \boldsymbol{P}_\Lambda}{2} |s_\Lambda\rangle$$

$$= \sum_{\mathcal{L}KK'LL'} \mathcal{M}(K,K',\mathcal{L};L,L') \left[\left[P_p^K \otimes P_\Lambda^{K'} \right]_{(\mathcal{L})} \otimes 4\pi \left[Y_L(\hat{\boldsymbol{p}}) \otimes Y_{L'}(\hat{\boldsymbol{p}}') \right]_{(\mathcal{L})} \right]_{(0)} . \tag{2.14}$$

Here we defined polarizations of rank 0 as $P_i^0 = 1$, and of rank 1 as $P_i^1 = (\boldsymbol{P})_i$.

$\mathcal{M}$ in Eq. (2.14) includes all the dynamical information of $p + n \to p + \Lambda$ reaction and is given by the partial wave T-matrix elements as

$$\begin{aligned}
\mathcal{M}(K,K',\mathcal{L};L,L') &= \frac{1}{2} \sum_{\mathcal{J}} \sqrt{[S][\bar{S}][S'][\bar{S}'][\ell][\bar{\ell}][\ell'][\bar{\ell}'][K][K'][\mathcal{L}]}[J][\bar{J}][\mathcal{J}] \\
&\times (-1)^{\ell+\bar{\ell}'+S+\bar{S}+S'+\bar{S}'+K+K'+L-\mathcal{L}-\mathcal{J}} (\ell 0 \bar{\ell} 0 | L 0)(\ell' 0 \bar{\ell}' 0 | L' 0) \\
&\times W(K \tfrac{1}{2} S \tfrac{1}{2}; \tfrac{1}{2} \bar{S}) W(K' \tfrac{1}{2} \bar{S}' \tfrac{1}{2}; \tfrac{1}{2} S') W(LKL'K'; \mathcal{J}\mathcal{L}) \\
&\times \left\{ \begin{array}{ccc} J & \ell & S \\ \bar{J} & \bar{\ell} & \bar{S} \\ \mathcal{J} & L & K \end{array} \right\} \left\{ \begin{array}{ccc} J & \ell' & S' \\ \bar{J} & \bar{\ell}' & \bar{S}' \\ \mathcal{J} & L' & K' \end{array} \right\} \\
&\times \langle [\ell' \otimes S']^M_{(J)}; p' | \frac{1}{4\pi} T | [\ell \otimes S]^M_{(J)}; p \rangle \\
&\times \langle [\bar{\ell}' \otimes \bar{S}']^M_{(\bar{J})}; p' | \frac{1}{4\pi} T | [\bar{\ell} \otimes \bar{S}]^M_{(\bar{J})}; p \rangle^*
\end{aligned} \tag{2.15}$$

with $[J] = 2J + 1$.

2.2 Polarization observables

Using the general formula of Eq. (2.11) , we can express explicitly the polarization observables. At first we integrate out the direction of the outgoing particle. Then the cross section is explicitly given as

$$\sigma(E) = \int d\Omega \frac{d\sigma}{d\Omega} \tag{2.16}$$

$$\begin{aligned}
&= \sigma_{\rm tot} \Big(1 + \bar{A}_p \boldsymbol{P}_p \cdot \hat{\boldsymbol{p}}_i + \bar{A}_\Lambda \boldsymbol{P}_\Lambda \cdot \hat{\boldsymbol{p}}_i + \bar{A}^0_{p\Lambda} \boldsymbol{P}_p \cdot \boldsymbol{P}_\Lambda \\
&\qquad + \bar{A}^1_{p\Lambda} (\boldsymbol{P}_p \times \boldsymbol{P}_\Lambda) \cdot \hat{\boldsymbol{p}}_i + \bar{A}^2_{p\Lambda} \Big((\boldsymbol{P}_p \cdot \hat{\boldsymbol{p}}_i)(\boldsymbol{P}_\Lambda \cdot \hat{\boldsymbol{p}}_i) - \frac{1}{3} \boldsymbol{P}_p \cdot \boldsymbol{P}_\Lambda \Big) \Big) .
\end{aligned} \tag{2.17}$$

The total cross section with unpolarized baryon is given as

$$\sigma_{\rm tot} = 4\pi N \mathcal{M}(0,0,0;0,0) \equiv 4\pi N A_{\rm tot} . \tag{2.18}$$

The asymmetry parameters $\bar{A}_p$ and $\bar{A}_\Lambda$, which violate parity, are given as

$$\bar{A}_p = -\mathcal{M}(1,0,1;1,0)/A_{\rm tot} \ , \tag{2.19}$$

$$\bar{A}_\Lambda = -\mathcal{M}(0,1,1;1,0)/A_{\rm tot} \ . \tag{2.20}$$

The parity conserving double polarization observables, $\bar{A}^0_{p\Lambda}$ and $\bar{A}^2_{p\Lambda}$ are

$$\bar{A}^0_{p\Lambda} = -\frac{1}{\sqrt{3}}\mathcal{M}(1,1,0;0,0)/A_{\rm tot} \ , \tag{2.21}$$

$$\bar{A}^2_{p\Lambda} = \sqrt{\frac{3}{2}}\mathcal{M}(1,1,2;2,0)/A_{\rm tot} \ . \tag{2.22}$$

$$\tag{2.23}$$

$\bar{A}^1_{p\Lambda}$ which violates both T and P is given as

$$\bar{A}^1_{p\Lambda} = -\frac{i}{\sqrt{2}}\mathcal{M}(1,1,1;1,0)/A_{\rm tot}. \tag{2.24}$$

In addition to the total cross section, we have four independent T invariant observables and one observable which violates T.

At first, let us assume $\hat{\boldsymbol{p}}_i$ is the direction of the proton and Λ polarization, for which we take z axis. Asymmetry parameters A_p and A_Λ are given by the cross sections of two spin states denoted by $\uparrow$ and $\downarrow$ as

$$A_p = \frac{\sigma(p\uparrow(z)) - \sigma(p\downarrow(z))}{\sigma(p\uparrow(z)) + \sigma(p\downarrow(z))} \ , \tag{2.25}$$

$$A_\Lambda = \frac{\sigma(\Lambda\uparrow(z)) - \sigma(\Lambda\downarrow(z))}{\sigma(\Lambda\uparrow(z)) + \sigma(\Lambda\downarrow(z))} \ , \tag{2.26}$$

The double polarization provides two additional quantities $A^0_{p\Lambda}$ and $A^2_{p\Lambda}$. If we take the difference of the cross sections with both proton and Λ spins flipped.

$$A_{L1} \equiv \frac{\sigma_{\uparrow(z)\uparrow(z)} - \sigma_{\downarrow(z)\downarrow(z)}}{\sigma_{\uparrow(z)\uparrow(z)} + \sigma_{\downarrow(z)\downarrow(z)}} = \frac{\bar{A}_p + \bar{A}_\Lambda}{1 + \bar{A}^0_{p\Lambda} + \frac{2}{3}\bar{A}^2_{p\Lambda}} \ , \tag{2.27}$$

$$A_{L2} \equiv \frac{\sigma_{\uparrow(z)\downarrow(z)} - \sigma_{\downarrow(z)\uparrow(z)}}{\sigma_{\uparrow(z)\downarrow(z)} + \sigma_{\downarrow(z)\uparrow(z)}} = \frac{\bar{A}_p - \bar{A}_\Lambda}{1 - \bar{A}^0_{p\Lambda} - \frac{2}{3}\bar{A}^2_{p\Lambda}} \ . \tag{2.28}$$

Here we denote cross section with proton spin $\uparrow$ in the z axis and Λ spin $\downarrow$ as $\sigma_{\uparrow(z)\downarrow(z)}$. Another possibility is to fix one of the baryon's spin and to flip the spin of the other baryon. The

following asymmetry parameters A_{L3} and A_{L4} are given by keeping the proton spin in the z direction and by flipping spin of Λ:

$$A_{L3} \equiv \frac{\sigma_{\uparrow(z)\uparrow(z)} - \sigma_{\uparrow(z)\downarrow(z)}}{\sigma_{\uparrow(z)\uparrow(z)} + \sigma_{\uparrow(z)\downarrow(z)}} = \frac{\bar{A}_\Lambda + \bar{A}^0_{p\Lambda} + \frac{2}{3}\bar{A}^2_{p\Lambda}}{1 + \bar{A}_p}, \tag{2.29}$$

$$A_{L4} \equiv \frac{\sigma_{\downarrow(z)\uparrow(z)} - \sigma_{\downarrow(z)\downarrow(z)}}{\sigma_{\downarrow(z)\uparrow(z)} + \sigma_{\downarrow(z)\downarrow(z)}} = \frac{\bar{A}_\Lambda - \bar{A}^0_{p\Lambda} - \frac{2}{3}\bar{A}^2_{p\Lambda}}{1 - \bar{A}_p}. \tag{2.30}$$

If we keep the spin of Λ, we obtain A_{L5} and A_{L6}

$$A_{L5} \equiv \frac{\sigma_{\uparrow(z)\uparrow(z)} - \sigma_{\downarrow(z)\uparrow(z)}}{\sigma_{\uparrow(z)\uparrow(z)} + \sigma_{\downarrow(z)\uparrow(z)}} = \frac{\bar{A}_p + \bar{A}^0_{p\Lambda} + \frac{2}{3}\bar{A}^2_{p\Lambda}}{1 + \bar{A}_\Lambda}, \tag{2.31}$$

$$A_{L6} \equiv \frac{\sigma_{\uparrow(z)\downarrow(z)} - \sigma_{\downarrow(z)\downarrow(z)}}{\sigma_{\uparrow(z)\downarrow(z)} + \sigma_{\downarrow(z)\downarrow(z)}} = \frac{\bar{A}_p - \bar{A}^0_{p\Lambda} - \frac{2}{3}\bar{A}^2_{p\Lambda}}{1 - \bar{A}_\Lambda}. \tag{2.32}$$

We can also polarize spins perpendicular to the incident proton momentum (y). There exists such an observable as A_{T1}:

$$A_{T1} \equiv \frac{\sigma_{\uparrow(y)\uparrow(y)} - \sigma_{\uparrow(y)\downarrow(y)}}{\sigma_{\uparrow(y)\uparrow(y)} + \sigma_{\uparrow(y)\downarrow(y)}} = \bar{A}^0_{p\Lambda} - \frac{1}{3}\bar{A}^2_{p\Lambda} \ . \tag{2.33}$$

Finally the T non-invariant observable can be obtained by keeping the spin of the baryon in the x direction, and the spin of the other baryon in the y direction. For example, A_{T2} is defined as

$$A_{T2} \equiv \frac{\sigma_{\uparrow(y)\uparrow(x)} - \sigma_{\uparrow(y)\downarrow(x)}}{\sigma_{\uparrow(y)\uparrow(x)} + \sigma_{\uparrow(y)\downarrow(x)}} = -\bar{A}^1_{p\Lambda}. \tag{2.34}$$

The angular dependence of polarization observables is given by $\boldsymbol{P}_p$, $\boldsymbol{P}_\Lambda$, $\hat{\boldsymbol{p}}_i$ and $\hat{\boldsymbol{p}}_f$ as follows,

$$\begin{aligned}
\frac{d\sigma}{d\Omega}(E, \boldsymbol{P}^p, \boldsymbol{P}^\Lambda) &= \frac{d\sigma^0}{d\Omega}[\quad 1 \\
&+ \boldsymbol{P}_p \cdot [\hat{\boldsymbol{p}}_i A_{p1} + \hat{\boldsymbol{p}}_f A_{p2} + \hat{\boldsymbol{p}}_i \times \hat{\boldsymbol{p}}_f A_{p3}] \\
&+ \boldsymbol{P}_\Lambda \cdot [\hat{\boldsymbol{p}}_i A_{\Lambda 1} + \hat{\boldsymbol{p}}_f A_{\Lambda 2} + \hat{\boldsymbol{p}}_i \times \hat{\boldsymbol{p}}_f A_{\Lambda 3}] \\
&+ \boldsymbol{P}_p \times \boldsymbol{P}_\Lambda \cdot [\hat{\boldsymbol{p}}_i A^1_{p\Lambda 1} + \hat{\boldsymbol{p}}_f A^1_{p\Lambda 2} + \hat{\boldsymbol{p}}_i \times \hat{\boldsymbol{p}}_f A^1_{p\Lambda 3}] \\
&+ \boldsymbol{P}_p \cdot \boldsymbol{P}_\Lambda A^2_{p\Lambda 1} + \hat{\boldsymbol{p}}_i \cdot \boldsymbol{P}_p \hat{\boldsymbol{p}}_i \cdot \boldsymbol{P}_\Lambda A^2_{p\Lambda 2} + \hat{\boldsymbol{p}}_f \cdot \boldsymbol{P}_p \hat{\boldsymbol{p}}_f \cdot \boldsymbol{P}_\Lambda A^2_{p\Lambda 3} \\
&+ (\hat{\boldsymbol{p}}_i \cdot \boldsymbol{P}_p \hat{\boldsymbol{p}}_f \cdot \boldsymbol{P}_\Lambda + \hat{\boldsymbol{p}}_f \cdot \boldsymbol{P}_p \hat{\boldsymbol{p}}_i \cdot \boldsymbol{P}_\Lambda) A^2_{p\Lambda 4} \\
&+ (\hat{\boldsymbol{p}}_i \cdot \boldsymbol{P}_p \hat{\boldsymbol{p}}_i \times \hat{\boldsymbol{p}}_f \cdot \boldsymbol{P}_\Lambda + \hat{\boldsymbol{p}}_i \times \hat{\boldsymbol{p}}_f \cdot \boldsymbol{P}_p \hat{\boldsymbol{p}}_i \cdot \boldsymbol{P}_\Lambda) A^2_{p\Lambda 5}
\end{aligned}$$

	P	$\not{P}$
T	$A^1_{p\Lambda 3},\ A^2_{p\Lambda 1},\ A^2_{p\Lambda 2},\ A^2_{p\Lambda 3},\ A^2_{p\Lambda 4}$	$A_{p1}, A_{p2}, A_{\Lambda 1}, A_{\Lambda 2}$
$\not{T}$	$A_{p3}, A_{\Lambda 3}$	$A^1_{p\Lambda 1},\ A^1_{p\Lambda 2},\ A^2_{p\Lambda 5},\ A^2_{p\Lambda 6}$

Table 1: T and P transform properties

$$+ \quad (\hat{\boldsymbol{p}}_f \cdot \boldsymbol{P}_p \hat{\boldsymbol{p}}_i \times \hat{\boldsymbol{p}}_f \cdot \boldsymbol{P}_\Lambda + \hat{\boldsymbol{p}}_i \times \hat{\boldsymbol{p}}_f \cdot \boldsymbol{P}_p \hat{\boldsymbol{p}}_f \cdot \boldsymbol{P}_\Lambda) A^2_{p\Lambda 6}], \tag{2.35}$$

$$\frac{d\sigma^0}{d\Omega} = NA, \tag{2.36}$$

$$A = \sum_L (-)^L \sqrt{[L]} \mathcal{M}(0,0,0;L,L) P_L(x). \tag{2.37}$$

Asymmetry parameters A_{pi}, $A_{\Lambda i}$, $A_{p\Lambda i}$, $A^2_{p\Lambda i}$ are expressed in terms of $\mathcal{M}(K,K',\mathcal{L};L,L')$ as follows,

$$A_{pi} = \sum_{LL'} \left(-\frac{1}{\sqrt{3}}\right) \mathcal{Y}^i_{LL'}(x) \mathcal{M}(1,0,1;L,L')/A, \tag{2.38}$$

$$A_{\Lambda i} = \sum_{LL'} \left(-\frac{1}{\sqrt{3}}\right) \mathcal{Y}^i_{LL'}(x) \mathcal{M}(0,1,1;L,L')/A, \tag{2.39}$$

$$A^1_{p\Lambda i} = \sum_{LL'} \left(-\frac{i}{\sqrt{6}}\right) \mathcal{Y}^i_{LL'}(x) \mathcal{M}(1,1,1;L,L')/A, \tag{2.40}$$

with $i = 1$ to 3.

$$A^2_{p\Lambda 1} = \sum_{LL'} \left[\delta_{LL'} (-)^{L+1} \sqrt{\frac{[L]}{3}} P_L(x) \mathcal{M}(1,1,0;L,L') + \mathcal{Z}^1_{LL'}(x) \mathcal{M}(1,1,2;L,L') \right] /A, \tag{2.41}$$

$$A^2_{p\Lambda j} = \sum_{LL'} \mathcal{Z}^j_{LL'}(x) \mathcal{M}(1,1,2;L,L')/A, \tag{2.42}$$

In Eq. (2.42), $j = 2$ to 6. $P_L(x)$ are Legendre functions and x is $\hat{\boldsymbol{p}}_f \cdot \hat{\boldsymbol{p}}_i$. The functions $\mathcal{Y}^i_{LL'}(x)$ and $\mathcal{Z}^j_{LL'}(x)$ are given by $P_L(x)$ and its derivatives $P'_L(x)$ and $P''_L(x)$, and are given in Appendix A. T and P transformation properties of each asymmetry parameter are classified in table 1.

Although the angular dependence of cross section is shown in Eq. (2.35), it is convenient to redefine the asymmetry parameters by introducing the following coordinate system: The z axis is chosen as the direction of incident proton momentum,

$$\hat{z} = \hat{\boldsymbol{p}}_i. \tag{2.43}$$

The y-axis is perpendicular to the scattering plane as,

$$\hat{y} = \frac{\boldsymbol{p}_i \times \boldsymbol{p}_f}{|\boldsymbol{p}_i \times \boldsymbol{p}_f|} \tag{2.44}$$

and the x-axis on the scattering plane is given as,

$$\hat{x} = \hat{y} \times \hat{z}. \tag{2.45}$$

This choice of coordinate is particularly convenient for the reaction near threshold energy region.

With this coordinates, the differential cross section Eq. (2.11) with arbitrary initial and final polarizations are given in terms of asymmetries $\boldsymbol{A}^p$, $\boldsymbol{A}^\Lambda$ and polarization transfer $\overrightarrow{K}$, as

$$\frac{d\sigma}{d\Omega}(E, \boldsymbol{P}^p, \boldsymbol{P}^\Lambda) = \frac{d\sigma^0}{d\Omega}\left(1 + \sum_{i=xyz} P_i^p A_i^p + \sum_{j=xyz} P_j^\Lambda A_j^\Lambda + \sum_{i,j=xyz} P_i^p P_j^\Lambda K_{ij}\right) \tag{2.46}$$

where

$$A_x^p = A_2^p \sin\theta, \qquad A_y^p = A_3^p \sin\theta, \quad A_z^p = (A_1^p + A_2^p \cos\theta), \tag{2.47}$$

$$A_x^\Lambda = A_2^\Lambda \sin\theta, \qquad A_y^\Lambda = A_3^\Lambda \sin\theta, \quad A_z^\Lambda = (A_1^\Lambda + A_2^\Lambda \cos\theta), \tag{2.48}$$

and

$$\begin{aligned}
K_{xx} &= A_{p\Lambda 1}^2 + A_{p\Lambda 3}^2 \sin^2\theta, \\
K_{xy} &= A_{p\Lambda 1}^1 + A_{p\Lambda 2}^1 \cos\theta + A_{p\Lambda 6}^2 \sin^2\theta, \\
K_{xz} &= -A_{p\Lambda 3}^1 \sin\theta + A_{p\Lambda 3}^2 \sin\theta\cos\theta + A_{p\Lambda 4}^2 \sin\theta, \\
K_{yx} &= -A_{p\Lambda 1}^1 - A_{p\Lambda 2}^1 \cos\theta + A_{p\Lambda 6}^2 \sin^2\theta, \\
K_{yy} &= A_{p\Lambda 1}^2, \\
K_{yz} &= A_{p\Lambda 2}^1 \sin\theta + A_{p\Lambda 5}^2 \sin\theta + A_{p\Lambda 6}^2 \sin\theta\cos\theta, \\
K_{zx} &= A_{p\Lambda 3}^1 \sin\theta + A_{p\Lambda 3}^2 \sin\theta\cos\theta + A_{p\Lambda 4}^2 \sin\theta, \\
K_{zy} &= -A_{p\Lambda 2}^1 \sin\theta + A_{p\Lambda 5}^2 \sin\theta + A_{p\Lambda 6}^2 \sin\theta\cos\theta, \\
K_{zz} &= A_{p\Lambda 1}^2 + A_{p\Lambda 2}^2 + A_{p\Lambda 3}^2 \cos^2\theta + 2A_{p\Lambda 4}^2 \cos\theta.
\end{aligned} \tag{2.49}$$

2.3 Polarization observables in the threshold energy region

Near the threshold energy of the $NN \to \Lambda N$ reaction, we can consider only the S-wave final state. In this section, we restrict ourselves to only the ${}^1S_0$ and ${}^3S_1$ final ΛN states, and present explicit formula of polarization observables[51]. In this case, we have only 6 independent matrix elements to describe the $NN \to YN$ reaction. The relevant matrix elements are [20]

$$\begin{aligned}
a &= <^1S_0|\frac{1}{4\pi}\hat{T}|^1S_0, T=1, P=+1>, \\
b &= <^1S_0|\frac{1}{4\pi}\hat{T}|^3P_0, T=1, P=-1>, \\
c &= <^3S_1|\frac{1}{4\pi}\hat{T}|^3S_1, T=0, P=+1>, \\
d &= <^3S_1|\frac{1}{4\pi}\hat{T}|^3D_1, T=0, P=+1>, \\
e &= <^3S_1|\frac{1}{4\pi}\hat{T}|^1P_1, T=0, P=-1>, \\
f &= <^3S_1|\frac{1}{4\pi}\hat{T}|^3P_1, T=1, P=-1> .
\end{aligned} \tag{2.50}$$

Isospin of initial pn state is $T = 0$ or 1, and $P = \pm 1$ stands for the parity conserving and violating matrix elements respectively. Then, the T-matrix can be written as

$$\begin{aligned}
\hat{T} &= a\frac{1-\boldsymbol{\sigma}_p\cdot\boldsymbol{\sigma}_\Lambda}{4} - b\frac{1-\boldsymbol{\sigma}_p\cdot\boldsymbol{\sigma}_\Lambda}{8}(\boldsymbol{\sigma}_p-\boldsymbol{\sigma}_\Lambda)\cdot\hat{\boldsymbol{p}} + c\frac{3+\boldsymbol{\sigma}_p\cdot\boldsymbol{\sigma}_\Lambda}{4} \\
&\quad + d\frac{1}{2\sqrt{2}}(3\boldsymbol{\sigma}_p\cdot\hat{\boldsymbol{p}}\boldsymbol{\sigma}_\Lambda\cdot\hat{\boldsymbol{p}} - \boldsymbol{\sigma}_p\cdot\boldsymbol{\sigma}_\Lambda) + e\frac{\sqrt{3}(3+\boldsymbol{\sigma}_p\cdot\boldsymbol{\sigma}_\Lambda)}{8}(\boldsymbol{\sigma}_p-\boldsymbol{\sigma}_\Lambda)\cdot\hat{\boldsymbol{p}} - f\frac{\sqrt{6}}{4}(\boldsymbol{\sigma}_p+\boldsymbol{\sigma}_\Lambda)\cdot\hat{\boldsymbol{p}},
\end{aligned} \tag{2.51}$$

which can be compared with a similar expression for the weak decay of hypernuclei. Then asymmetry parameters defined in Eqs. (2.18) - (2.24) are simply expressed as

$$\bar{A} = \frac{1}{4}\left[|a|^2+|b|^2+3(|c|^2+|d|^2+|e|^2+|f|^2])\right], \tag{2.52}$$

$$\bar{A}_p = \frac{1}{4}2\sqrt{3}Re\left[-ab^*/\sqrt{3}+e(c-\sqrt{2}d)^* - f(\sqrt{2}c+d)^*\right]/\bar{A}, \tag{2.53}$$

$$\bar{A}_\Lambda = \frac{1}{4}2\sqrt{3}Re\left[-ae^*+b(c-\sqrt{2}d)^*/\sqrt{3} - f(\sqrt{2}c+d)^*\right]/\bar{A}, \tag{2.54}$$

$$\bar{A}^0_{p\Lambda} = \frac{1}{4}2Re\left[-ac^*+|c|^2-\frac{1}{2}|d|^2+\frac{1}{\sqrt{3}}b(e+\sqrt{2}f)^* + f(\sqrt{2}e+\frac{1}{2}f)^*\right]/\bar{A}, \tag{2.55}$$

$$\bar{A}^1_{p\Lambda} = \frac{1}{4}\sqrt{6}Im\left[af^* - (b/\sqrt{3}+e)(\sqrt{2}c+d)^* + f(c-\sqrt{2}d)^*\right]/\bar{A}, \quad (2.56)$$

$$\bar{A}^2_{p\Lambda} = \frac{1}{4}3\sqrt{2}Re\left[ad^* + (b/\sqrt{3}-f/\sqrt{2})(\sqrt{2}e-f)^* + d(c+d/\sqrt{2})^*\right]/\bar{A}. \quad (2.57)$$

Since we restrict ourselves to the S-wave ΛN state, These parameters are related with A_{p1}, $A_{\Lambda 1}$, $A^1_{p\Lambda 1}$, $A^2_{p\Lambda 1}$, $A^2_{p\Lambda 2}$, which have no angular dependence. The relation between $\bar{A}$ and A are

$$A = \bar{A}, \quad (2.58)$$

$$A_{p1} = \bar{A}_p, \quad (2.59)$$

$$A_{\Lambda 1} = \bar{A}_\Lambda, \quad (2.60)$$

$$A^1_{p\Lambda 1} = \bar{A}^1_{p\Lambda}, \quad (2.61)$$

$$A^2_{p\Lambda 1} = \bar{A}^0_{p\Lambda} - \bar{A}^2_{p\Lambda}/3, \quad (2.62)$$

$$A^2_{p\Lambda 2} = \bar{A}^2_{p\Lambda}. \quad (2.63)$$

All other A vanish. Expression of angular distribution in Eq. (2.35) is simply the total cross section divided by 4π.

It is noticed $\bar{A}_\Lambda$ corresponds to the asymmetry parameter (α_p) from the polarized hypernuclei which has been experimentally measured[17]. Asymmetric emission of proton from polarized hypernuclei is represented as

$$W(\theta) = 1 + \alpha_p \cos\theta. \quad (2.64)$$

As an example, the asymmetry parameter α_p for the ${}^5_\Lambda$He $\to p + n + {}^3$H is given as

$$\alpha_p = \frac{2\sqrt{3}Re[-\bar{a}\bar{e}^* + \bar{b}(\bar{c}-\sqrt{2}\bar{d})^*/\sqrt{3} - \bar{f}(\sqrt{2}\bar{c}+\bar{d})^*]}{|\bar{a}|^2 + |\bar{b}|^2 + 3(|\bar{c}|^2 + |\bar{d}|^2 + |\bar{e}|^2 + |\bar{f}|^2)}, \quad (2.65)$$

where $\bar{i}(i = a, b, ..f)$ are matrix elements for the NM-decay similar to Eq. (2.51). Here we assume simply the $(0s)^5$ configuration of ${}^5_\Lambda$He. Eq. (2.65) shows, α_p is equivalent to $\bar{A}_\Lambda$ for this reaction. It is noticed that the interference term between spin singlet and triplet ΛN matrix elemetnts is missing in the commonly used formula[52]. Although it is clear that spin singlet state gives no asymmetry, the ΛN system buried in hypernuclei can be spin-singlet and triplet states whose interference results in the above formula.

3 The $pn \to p\Lambda$ Transition Potential

3.1 Meson exchange model of weak $NN \to \Lambda N$ potential

We adopt meson-exchange model of strangeness changing weak BB interaction. In the study of non-mesic weak decay of Λ-hypernuclei, various meson-exchange models have been proposed. In this paper, we include pseudo-scalar meson (π, η, K) and vector meson (ρ, ω, K^*) exchange processes in the one boson exchange model. Since the strong interaction conserves strangeness, one of the meson-baryon vertices in the potential should be the weak interaction.

By using a model Hamiltonian of strong and weak meson-baryon interactions, the weak $N + N \to N + \Lambda$ transition potential is constructed with the static approximation for the meson propagator, and also the baryon masses are assumed to be large compared with typical momentum of this reaction. These approximations may be accepted for the first study of this reaction and for our purpose to clarify the role of polarization observables in the study of weak BB interaction. It should be kept in mind that both two assumptions may be questionable and should be examined in the future study: A free Λ can decay into a nucleon by emitting a real pion. Therefore, the static approximation neglecting the retardation of pion propagator might affect the range of potential with pion-exchange. The momentum of final nucleon is 400MeV/c which is roughly half of baryons mass, $p/M \sim \frac{1}{2}$.

Here we will not consider $pn \to N\Sigma$ process, since its effect has been estimated to be an order of magnitude smaller than the $p + n \to p + \Lambda$ process.

3.1.1 Pseudoscalar meson-exchange potential

The weak non-leptonic decay of Λ is parameterized as

$$\mathcal{H}^W_\Lambda = iG_F m_\pi^2 \bar{\Psi}_N (A_\pi + B_\pi \gamma_5) \boldsymbol{\tau} \binom{0}{1} \Psi_\Lambda \boldsymbol{\phi_\pi} \tag{3.1}$$

where Ψ_N, Ψ_Λ and ϕ_π are the nucleon, Λ and pion fields respectively. The spurion spinor $\binom{0}{1}$ is introduced in the Hamiltonian in Eq. (3.1) to guarantee the $\Delta I = \frac{1}{2}$ rule. A_π and B_π are determined from the decay rate and asymmetry parameter of the free Λ decay. With

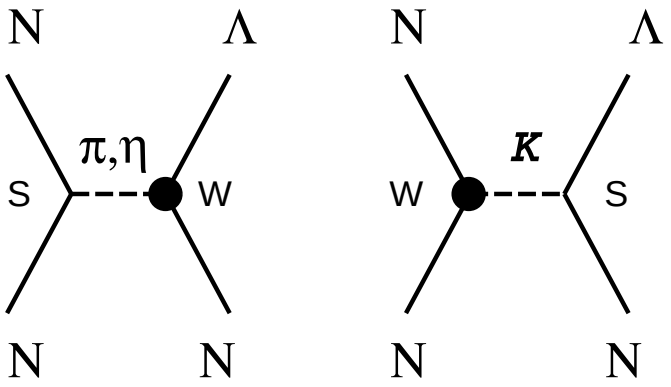

Figure 1: Feynman graph for pseudoscalar meson exchange

$G_F m_\pi^2 = 2.21 \times 10^{-7}$, A_π and B_π are given as

$$A_\pi = 1.05, \quad B_\pi = -7.15. \tag{3.2}$$

By assuming CP invariance we can construct a Hamiltonian for the $p + n \to p + \Lambda$ reaction as

$$\mathcal{H}^W_{N\Lambda\pi} = iG_F m_\pi^2 \bar{\Psi}_\Lambda(_{0,1})(-A_\pi + B_\pi \gamma_5)\boldsymbol{\tau}\Psi_N \boldsymbol{\phi_\pi} \tag{3.3}$$

where we assumed A_π and B_π are effective coupling constants. For the following weak meson-baryon Hamiltonian, we also adopt the same procedure.

The strong πNN vertex is given as

$$\mathcal{H}^S_{NN\pi} = ig_{NN\pi}\bar{\Psi}_N \gamma_5 \boldsymbol{\tau}\Psi_N \boldsymbol{\phi_\pi} \tag{3.4}$$

By using Eqs. (3.3) and (3.4) with the non-relativistic approximation, the standard procedure gives pion-exchange potential V_W as

$$V_\pi(\boldsymbol{p}', \boldsymbol{p}) = -\frac{1}{(2\pi)^3} G_F m_\pi^2 \frac{g}{2m_N} \boldsymbol{\sigma}_1 \cdot (\boldsymbol{p} - \boldsymbol{p}') \left(\hat{A} + \hat{B} \left(\frac{\boldsymbol{\sigma}_2 \cdot \boldsymbol{p}}{2m_N} - \frac{\boldsymbol{\sigma}_2 \cdot \boldsymbol{p}'}{2m_\Lambda} \right) \right) \frac{1}{(\boldsymbol{p} - \boldsymbol{p}')^2 + \mu^2}. \tag{3.5}$$

Here we assigned Λ in the final state to particle 2 with momentum $-\boldsymbol{p}'$. Here, the parameters are chosen as

$$g \;=\; g_{NN\pi}, \tag{3.6}$$

$$\hat{A} = A_\pi(\boldsymbol{\tau}_1 \cdot \boldsymbol{\tau}_2), \tag{3.7}$$

$$\hat{B} = B_\pi(\boldsymbol{\tau}_1 \cdot \boldsymbol{\tau}_2), \tag{3.8}$$

$$\mu = m_\pi. \tag{3.9}$$

The $\hat{A}$ and $\hat{B}$ terms in V_π are parity-violating(PV) and parity-conserving(PC) potential respectively.

For the η meson exchange, we used the following strong and weak Hamiltonian,

$$\mathcal{H}^W_{N\Lambda\eta} = iG_F m_\pi^2 \bar{\Psi}_\Lambda {}_{(0,1)}(-A_\eta + B_\eta\gamma_5)\Psi_N\phi_\eta, \tag{3.10}$$

$$\mathcal{H}^S_{NN\eta} = ig_{NN\eta}\bar{\Psi}_N\gamma_5\Psi_N\phi_\eta, \tag{3.11}$$

$$\tag{3.12}$$

The η exchange weak potential is given by the following redefinition of the coupling constants and mass in Eq. (3.5) as

$$g = g_{NN\eta}, \tag{3.13}$$

$$\hat{A} = A_\eta, \tag{3.14}$$

$$\hat{B} = B_\eta, \tag{3.15}$$

$$\mu = m_\eta. \tag{3.16}$$

Here, the coupling constants of weak decay with other mesons should be determined by assuming any model. They will be discussed in the next section.

For the kaon exchange, the weak and strong Hamiltonians are given as

$$\begin{aligned}\mathcal{H}^W_{NNK} = iG_F m_\pi^2 \Big[&\bar{\Psi}_N\phi^K(-C_K^{\rm PV} + C_K^{\rm PC}\gamma_5)_{(0,1)}\Psi_N, \\ &+({}_{(0,1)}\phi^K)\bar{\Psi}_N(-D_K^{\rm PV} + D_K^{\rm PC}\gamma_5)\Psi_N\Big],\end{aligned} \tag{3.17}$$

$$\mathcal{H}^S_{\Lambda NK} = ig_{\Lambda NK}\bar{\Psi}_\Lambda(\phi^K)^\dagger\gamma_5\Psi_N. \tag{3.18}$$

Here the weak Hamiltonian consists of two terms C and D corresponding to different coupling scheme of flavor structure. ϕ^K and $(\phi^K)^\dagger$ are defined as

$$\phi^K = \begin{pmatrix}\phi^{K^+} \\ \phi^{K^0}\end{pmatrix}, \tag{3.19}$$

$$(\phi^K)^\dagger = (\phi^{K^-}, \phi^{\bar{K}^0}). \tag{3.20}$$

Since kaons carry strangeness, kaon-exchange potential is given as

$$V_K(\boldsymbol{p}',\boldsymbol{p}) = -\frac{1}{(2\pi)^3}G_F m_\pi^2 g_{\Lambda NK}\left(\hat{A} - \frac{\hat{B}}{2m_N}(\boldsymbol{\sigma}_1\cdot(\boldsymbol{p}-\boldsymbol{p}'))\right)\boldsymbol{\sigma}_2\cdot(\frac{\boldsymbol{p}'}{2m_\Lambda} - \frac{\boldsymbol{p}}{2m_N})\frac{1}{(\boldsymbol{p}-\boldsymbol{p}')^2+m_K^2} \tag{3.21}$$

where

$$\hat{A} = \frac{C_K^{\rm PV}}{2} + D_K^{\rm PV} + C_K^{\rm PV}\boldsymbol{\tau}_1\cdot\boldsymbol{\tau}_2, \tag{3.22}$$

$$\hat{B} = \frac{C_K^{\rm PC}}{2} + D_K^{\rm PC} + C_K^{\rm PC}\boldsymbol{\tau}_1\cdot\boldsymbol{\tau}_2. \tag{3.23}$$

Here we assumed that baryon 1 feels the weak interaction, while baryon 2 feels the strong interaction as shown in Fig. 1

3.1.2 Vector meson-exchange potential

The weak $\Lambda N\rho$ and strong $NN\rho$ vertices are given as Ref. [28]

$$\mathcal{H}^W_{N\Lambda\rho} \equiv G_F m_\pi^2 \bar{\Psi}_{\Lambda(0,1)}\left(\alpha\gamma^\mu\boldsymbol{\rho}_\mu - \frac{\beta}{2\bar{m}}\sigma^{\mu\nu}\partial_\nu\boldsymbol{\rho}_\mu + \varepsilon\gamma^\mu\gamma^5\boldsymbol{\rho}_\mu\right)\boldsymbol{\tau}\Psi_N, \tag{3.24}$$

$$\mathcal{H}^S_{NN\rho} \equiv \bar{\Psi}_N\left(g^V_{NN\rho}\gamma^\mu\boldsymbol{\rho}_\mu - \frac{g^T_{NN\rho}}{2m}\sigma^{\mu\nu}\partial_\nu\boldsymbol{\rho}_\mu\right)\boldsymbol{\tau}\Psi_N. \tag{3.25}$$

The CP invariance requires the same form for both $\Lambda\to N\rho$ and $N\to\Lambda\rho$ weak Hamiltonians.

The weak ρ-exchange potential is given as

$$\begin{aligned} V_\rho(\boldsymbol{p}',\boldsymbol{p}) = {} & \frac{1}{(2\pi)^3}G_F m_\pi^2\Big[F_1\hat{\alpha} - \frac{(\hat{\alpha}+\hat{\beta})(F_1+F_2)}{2m_N}(\boldsymbol{\sigma}_1\times(\boldsymbol{p}-\boldsymbol{p}'))\cdot(\boldsymbol{\sigma}_2\times(\frac{\boldsymbol{p}}{2m_N} - \frac{\boldsymbol{p}'}{2m_\Lambda})) \\ & - i\frac{\hat{\epsilon}(F_1+F_2)}{2m_N}(\boldsymbol{\sigma}_1\times\boldsymbol{\sigma}_2)\cdot(\boldsymbol{p}-\boldsymbol{p}')\Big]\frac{1}{(\boldsymbol{p}-\boldsymbol{p}')^2+\mu^2} \end{aligned} \tag{3.26}$$

with

$$F_1 = g^V_{NN\rho}, \tag{3.27}$$

$$F_2 = g^T_{NN\rho}, \tag{3.28}$$

$$\hat{\alpha} = \alpha_\rho\boldsymbol{\tau}_1\cdot\boldsymbol{\tau}_2,$$

$$\hat{\beta} = \beta_\rho\boldsymbol{\tau}_1\cdot\boldsymbol{\tau}_2,$$

$$\hat{\epsilon} = \epsilon_\rho\boldsymbol{\tau}_1\cdot\boldsymbol{\tau}_2,$$

$$\mu = m_\rho. \tag{3.29}$$

Here it is noticed that the non-local part proportional to $\boldsymbol{p}+\boldsymbol{p}'$ is neglected. Since β and F_2 are larger than α and F_1, this approximation may be justified.

Terms proportional to α and β are PC potentials and ϵ term is the PV potential. Although PC part consists of spin-spin and tensor potential as a consequence of pseudoscalar-meson-exchange potential, the spin structure of PV potential $(i\boldsymbol{\sigma}_1 \times \boldsymbol{\sigma}_2 \cdot \boldsymbol{q})$ is quite different from pseudoscalar-meson-exchange potential, which is true for all vector meson exchange potentials. It is noticed that we found PV potential in the literature[28, 33] gives opposite sign against our expression, while our formula agree with [29, 32]. This leads us to different conclusion on the magnitude of PV matrix elements.

The weak and strong Hamiltonians for ω meson are given as

$$\mathcal{H}^W_{N\Lambda\omega} \equiv G_F m_\pi^2 \bar{\Psi}_\Lambda {}_{(0,1)} \left(\alpha\gamma^\mu\omega_\mu - \frac{\beta}{2\bar{m}}\sigma^{\mu\nu}\partial_\nu\omega_\mu + \varepsilon\gamma^\mu\gamma^5\omega_\mu\right)\Psi_N, \tag{3.30}$$

$$\mathcal{H}^S_{NN\omega} \equiv \bar{\Psi}_\Lambda \left(g^V_{NN\omega}\gamma^\mu\omega_\mu - g^T_{NN\omega}\frac{\sigma^{\mu\nu}}{2m}\partial_\nu\omega_\mu\right)\Psi_N. \tag{3.31}$$

$$\tag{3.32}$$

The ω meson exchange weak potential V_ω is given by the following replacement on V_ρ

$$\mu = m_\omega, \tag{3.33}$$

$$F_1 = g^V_{NN\omega}, \tag{3.34}$$

$$F_2 = g^T_{NN\omega}, \tag{3.35}$$

$$\hat{\alpha} = \alpha_\omega, \tag{3.36}$$

$$\hat{\beta} = \beta_\omega, \tag{3.37}$$

$$\hat{\epsilon} = \epsilon_\omega. \tag{3.38}$$

The Hamiltonian for K^* is given as

$$\begin{aligned}\mathcal{H}^W_{NNK^*} \equiv\ & G_F m_\pi^2 \left(\left(C^{PC,V}_{K^*}\bar{\Psi}_N\begin{pmatrix}0\\1\end{pmatrix}(K^*_\mu)^\dagger\gamma^\mu\Psi_N + D^{PC,V}_{K^*}\bar{\Psi}_N\gamma^\mu\Psi_N(K^*_\mu)^\dagger\begin{pmatrix}0\\1\end{pmatrix}\right)\right. \\ & - \left(C^{PC,T}_{K^*}\bar{\Psi}_N\begin{pmatrix}0\\1\end{pmatrix}\partial_\nu(K^*_\mu)^\dagger\tfrac{\sigma^{\mu\nu}}{2m}\Psi_N + D^{PC,T}_{K^*}\bar{\Psi}_N\tfrac{\sigma^{\mu\nu}}{2m}\Psi_N\partial_\nu(K^*_\mu)^\dagger\begin{pmatrix}0\\1\end{pmatrix}\right) \\ & \left. + \left(C^{PV}_{K^*}\bar{\Psi}_N\begin{pmatrix}0\\1\end{pmatrix}(K^*_\mu)^\dagger\gamma^\mu\gamma_5\Psi_N + D^{PV}_{K^*}\bar{\Psi}_N\gamma^\mu\gamma_5\Psi_N(K^*_\mu)^\dagger\begin{pmatrix}0\\1\end{pmatrix}\right)\right),\end{aligned} \tag{3.39}$$

$$\mathcal{H}^S_{\Lambda NK^*} \equiv \bar{\Psi}_\Lambda \left(g^V_{\Lambda NK^*}\gamma^\mu(K^*{}_\mu)^\dagger - g^T_{\Lambda NK^*}\frac{\sigma^{\mu\nu}}{2m}(\partial_\nu K^*{}_\mu)^\dagger\right)\Psi_N. \tag{3.40}$$

The K^*-exchange weak potential is given as follows:

$$
\begin{aligned}
V_{K^*}(\boldsymbol{p}',\boldsymbol{p}) &= \frac{G_F m_\pi^2}{(2\pi)^3}\left[g^V_{NNK^*}\hat{\alpha}_{K^*} - \frac{g^V_{NNK^*}(\hat{\alpha}_{K^*}+\hat{\beta}_{K^*})}{2m}\boldsymbol{\sigma}_1\times(\boldsymbol{p}'-\boldsymbol{p})\boldsymbol{\sigma}_2\times\left(\frac{\boldsymbol{p}'}{2m_\Lambda}-\frac{\boldsymbol{p}}{2m}\right)\right. \\
&\quad - \frac{g^T_{NNK^*}(\hat{\alpha}_{K^*}+\hat{\beta}_{K^*})}{4m^2}\boldsymbol{\sigma}_1\times(\boldsymbol{p}'-\boldsymbol{p})\boldsymbol{\sigma}_2\times(\boldsymbol{p}'-\boldsymbol{p}) \\
&\quad \left. + \hat{\epsilon}_{K^*}g^V_{NNK^*}i\boldsymbol{\sigma}_1\times\boldsymbol{\sigma}_2\cdot\left(\frac{\boldsymbol{p}'}{2m_\Lambda}-\frac{\boldsymbol{p}}{2m}\right) + \frac{\hat{\epsilon}_{K^*}g^T_{NNK^*}}{2m}i\boldsymbol{\sigma}_1\times\boldsymbol{\sigma}_2\cdot(\boldsymbol{p}'-\boldsymbol{p})\right] \qquad (3.41)
\end{aligned}
$$

with

$$
\begin{aligned}
\hat{\alpha}_{K^*} &= \frac{C^{PC,V}_{K^*}}{2} + D^{PC,V}_{K^*} + \frac{C^{PC,V}_{K^*}}{2}\boldsymbol{\tau}_1\cdot\boldsymbol{\tau}_2, \qquad (3.42)\\
\hat{\beta}_{K^*} &= \frac{C^{PC,T}_{K^*}}{2} + D^{PC,T}_{K^*} + \frac{C^{PC,T}_{K^*}}{2}\boldsymbol{\tau}_1\cdot\boldsymbol{\tau}_2, \qquad (3.43)\\
\hat{\epsilon}_{K^*} &= \frac{C^{PV}_{K^*}}{2} + D^{PV}_{K^*} + \frac{C^{PV}_{K^*}}{2}\boldsymbol{\tau}_1\cdot\boldsymbol{\tau}_2. \qquad (3.44)
\end{aligned}
$$

We use the same monopole form factor

$$
F(\boldsymbol{p}',\boldsymbol{p}) = \frac{\Lambda_i^2-\mu_i^2}{\Lambda_i^2+(\boldsymbol{p}'-\boldsymbol{p})^2} \qquad (3.45)
$$

at the strong and the weak vertices, where the cutoff parameter Λ_i depends on the exchanged meson i.

3.2 Weak coupling constants

Among various required weak meson-baryon Hamiltonians, only the $\pi N\Lambda$ weak interaction can be determined from the experimental data of the non-leptonic Λ decay. We follow the procedure of Refs. [32, 33] to determine the interaction for other mesons. We briefly summarize their results on PV and PC weak interaction.

3.2.1 Parity-violating amplitude

The soft meson reduction theory gives the weak PV interaction of pseudoscalar meson emission as

$$
\lim_{q\to 0}\langle B'M_i(q)|H_{PV}|B\rangle = -\frac{i}{F_\pi}\langle B'|[F_i^5,H_{PV}]|B\rangle \qquad (3.46)
$$

Here q is the momentum of the meson, and F_i is an SU(3) generator. Assuming the current algebra it reduces to

$$\lim_{q\to 0}\langle B' M_i(q)|H_{PV}|B\rangle = -\frac{i}{F_\pi}\langle B'|[F_i, H_{PC}]|B\rangle. \tag{3.47}$$

Here the lightest spin $\frac{1}{2}$ baryons and 0^- pseudoscalar mesons are assumed to belong to an octet representation of flavor SU(3). Furthermore the weak Hamiltonian H_W is assumed to transform like a 6th component of octet,

$$\langle B_k|H_w^6|B_j\rangle = iF f_{6jk} + Dd_{6jk}, \tag{3.48}$$

where f_{ijk} and d_{ijk} are the SU(3) coefficients, and F and D the reduced matrix elements. Then the matrix elements of weak Hamiltonian of necessary pseudoscalar meson are given in term of non-leptonic decay of a hyperon into a pion and a nucleon as

$$\langle nK^0|H_{\rm pv}|n\rangle = \sqrt{\frac{3}{2}}\Lambda_-^0 - \frac{1}{\sqrt{2}}\Sigma_0^+, \tag{3.49}$$

$$\langle pK^0|H_{\rm pv}|p\rangle = -\sqrt{2}\Sigma_0^+, \tag{3.50}$$

$$\langle nK^+|H_{\rm pv}|p\rangle = \sqrt{\frac{3}{2}}\Lambda_-^0 + \frac{1}{\sqrt{2}}\Sigma_0^+, \tag{3.51}$$

$$\langle n\eta|H_{\rm pv}|\Lambda\rangle = \sqrt{\frac{3}{2}}\Lambda_-^0, \tag{3.52}$$

where Λ_-^0 stands for $\langle p\pi^-|H_{PV}|\Lambda\rangle$, and, Σ_0^+, for $\langle p\pi^0|H_{PV}|\Sigma^+\rangle$. The same relations as above hold for the hyperon decay with emission of other pseudoscalar mesons.

The SU(3) symmetry alone does not predict PV coupling constants for vector mesons. The higher symmetry $SU(6)_W$, however, enables us to relate the PV coupling constants of vector mesons with those of pion. The $SU(6)_W$ tensor structure of the weak Hamiltonian is given by using the current-current form of the weak Hamiltonian in term of quark fields[53]. The PV coupling constants of vector mesons are expressed as

$$A_\pi = \frac{1}{\sqrt{2}}\Lambda_-^0, \tag{3.53}$$

$$A_\eta = \sqrt{\frac{3}{2}}\Lambda_-^0, \tag{3.54}$$

$$C_{\rm K}^{\rm PV} = \sqrt{\frac{3}{2}}\Lambda_-^0 + \frac{1}{\sqrt{2}}\Sigma_0^+, \tag{3.55}$$

$$D_{\rm K}^{\rm PV} = -\sqrt{2}\Sigma_0^+, \tag{3.56}$$

$$\varepsilon_\rho = \frac{2}{3}\Lambda_-^0 - \frac{1}{\sqrt{3}}\Sigma_0^+ + \sqrt{3}a_T, \tag{3.57}$$

$$\varepsilon_\omega = \Sigma_0^+ - \frac{1}{3}a_T, \tag{3.58}$$

$$C_{\rm K^*}^{\rm PV} = -\sqrt{3}\Lambda_-^0 + \frac{1}{3}\Sigma_0^+ + \frac{10}{3}a_T, \tag{3.59}$$

$$D_{\rm K^*}^{\rm PV} = -\frac{2}{3}\Sigma_0^+ + \frac{8}{9}a_T. \tag{3.60}$$

where additional parameter a_T appears in the coupling constants for the vector mesons. We assume $G_F m_\pi^2 a_T = -0.953 \times 10^{-7}$, following Ref [33].

Here it is noticed that $\mathrm{SU}(6)_W$ symmetry relates the PV coupling constants of pseudoscalar and vector mesons, which fixes phase relations between them. Our meson-exchange weak interaction V_W includes the strong and weak interaction Hamiltonians. It is not clear whether the phase relations between pseudoscalar and vector meson for the strong interaction Hamiltonian, is the same as those $\mathrm{SU}(6)_W$. Therefore, we still have phase ambiguities of the PV part of pseudoscalar and vector meson exchange potential.

3.2.2 Parity-conserving amplitude

One of the method to derive PC amplitude is the so called pole model. We assumed the PC baryon-baryon-meson(BBM) amplitude is dominated by the $\frac{1}{2}^+$ baryon pole term, as schematically shown in Fig. 2. Vertices S and W in the figure denote strong and weak interaction vertices respectively. Therefore, the PC amplitude is given by the strong BBM coupling constants and matrix element of weak PC interaction between baryons.

$$g_{BB'M} = \sum_{B''} A_{BB''} \frac{1}{m_B - m_{B''}} g_{B''B'M} + g_{BB''M} \frac{1}{m_{B'} - m_{B''}} A_{B''B'}. \tag{3.61}$$

Required baryon matrix elements of PC weak interaction is given by the PV non-leptonic decay of hyperon as

$$\lim_{q\to 0}\langle \pi^0 n|H_{\rm pv}|\Lambda\rangle = \frac{-i}{F_\pi}\langle n|[F_{\pi^0}^5, H_{\rm pv}]|\Lambda\rangle = \frac{i}{2F_\pi}\langle n|H_{\rm pc}|\Lambda\rangle,$$

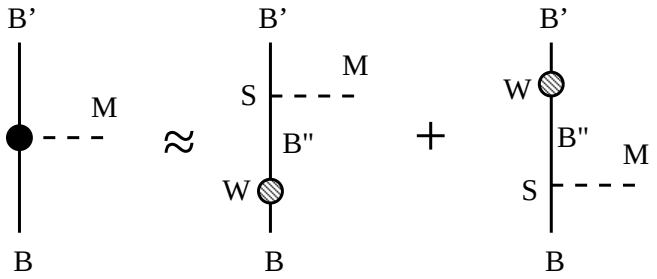

Figure 2: Schematic representation of pole model. S stands for strong vertex, W for weak transition vertex respectively

and

$$\lim_{q\to 0}\langle \pi^0 p|H_{\rm pv}|\Sigma^+\rangle \;=\; \frac{-i}{F_\pi}\langle p|[F^5_{\pi^0},H_{\rm pv}]|\Sigma^+\rangle = \frac{i}{2F_\pi}\langle p|H_{\rm pc}|\Sigma^+\rangle\ . \tag{3.62}$$

The pole model gives PC weak meson-exchange potential as shown in Figure 3.

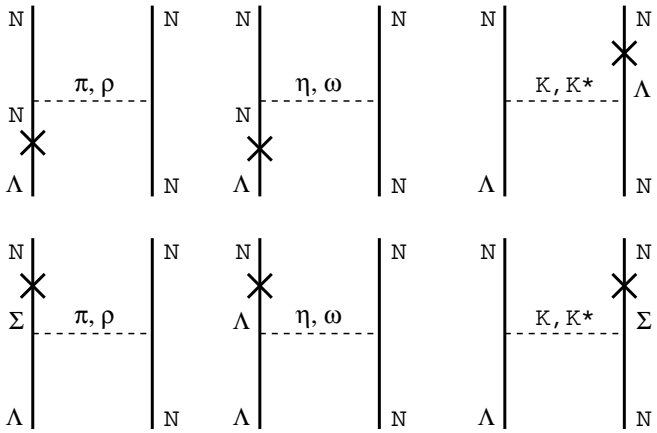

Figure 3: Weak BB interaction in the pole model

It is noticed that there are no phase ambiguities in the PC potentials V_W^{PC}, since they are given by the square of strong interaction coupling constants.

We summarize numerical values of coupling constants in the table 2.

Table 2: Weak and strong coupling constants. Coupling constants for strong interaction are taken from Nijmegen potential [5], while vertex functions are taken from Jülich potential[8].

Meson	Strong CC	Weak CC		Λ_i
		PC	PV	(GeV)
π	$g_{\mathrm{NN}\pi} = 13.3$	$B_\pi = -7.15$	$A_\pi = 1.05$	1.30
η	$g_{\mathrm{NN}\eta} = 6.40$	$B_\eta = -14.3$	$A_\eta = 1.80$	1.30
K	$g_{\Lambda\mathrm{NK}} = -14.1$	$C_{\mathrm{K}}^{\mathrm{PC}} = -18.9$	$C_{\mathrm{K}}^{\mathrm{PV}} = 0.76$	1.20
		$D_{\mathrm{K}}^{\mathrm{PC}} = 6.63$	$D_{\mathrm{K}}^{\mathrm{PV}} = 2.09$	
ρ	$g_{\mathrm{NN}\rho}^{\mathrm{V}} = 3.16$	$\alpha_\rho = -3.50$	$\varepsilon_\rho = 1.09$	1.40
	$g_{\Lambda\Sigma\rho}^{\mathrm{T}} = 13.3$	$\beta_\rho = -6.11$		
ω	$g_{\mathrm{NN}\omega}^{\mathrm{V}} = 10.5$	$\alpha_\omega = -3.69$	$\varepsilon_\omega = -1.33$	1.50
	$g_{\mathrm{NN}\omega}^{\mathrm{T}} = 3.22$	$\beta_\omega = -8.04$		
K*	$g_{\Lambda\mathrm{NK}^*}^{\mathrm{V}} = -5.47$	$C_{\mathrm{K}^*}^{\mathrm{PC,V}} = -3.61$	$C_{\mathrm{K}^*}^{\mathrm{PV}} = -4.48$	2.20
	$g_{\Lambda\mathrm{NK}^*}^{\mathrm{T}} = -11.9$	$C_{\mathrm{K}^*}^{\mathrm{PC,T}} = -17.9$		
		$D_{\mathrm{K}^*}^{\mathrm{PC,V}} = -4.89$	$D_{\mathrm{K}^*}^{\mathrm{PV}} = 0.60$	
		$D_{\mathrm{K}^*}^{\mathrm{PC,T}} = 9.30$		

Table 3: Mass parameters

Particle	mass(MeV)
p	938.3
n	939.6
Λ	1115.6
π	139
η	547
K	493
ρ	770
ω	782
K^*	892

4 Results and Discussion

In this section we briefly discuss the BB wave function in momentum space. Then we present our numerical results on the energy dependence of total cross section and polarization observables. We will give simple arguments to understand the mechanism of polarization in $p + n \to p + \Lambda$ reaction. Finally the angular distribution of polarization observables is discussed.

4.1 NN and ΛN distorted wave

The initial (pn) and final (Λp) scattering wave functions are obtained by solving the following Lippmann-Schwinger equations,

$$|\chi_i^{(+)}\rangle = |\phi_i\rangle + \frac{1}{E_{NN} - H_{0NN} - V_{NN} + i\epsilon} V_{NN} |\phi_i\rangle \tag{4.1}$$

and

$$\langle\chi_f^{(-)}| = \langle\phi_f| + \langle\phi_f| V_{YN} \frac{1}{E_{YN} - H_{0YN} - V_{YN} + i\epsilon}. \tag{4.2}$$

Here $|\phi_i\rangle$ and $\langle\phi_f|$ are incoming (pn) and outgoing (Λp) plane waves. By using the partial wave expansion, the NN equation is reduced into the coupled equations of at most two channels, while, the YN equation, the coupled channel equation of six channels due to the tensor force and three kinds of Fock space. Here we briefly explain the standard method for solving Lippmann-Schwinger equation in momentum space. We show only the case with no channel coupling. Its extension to the many channel case is obvious.

At first, we introduce the T-matrix for the elastic NN (or YN) scattering for channel α. α denote the spin orbital and total angular momentum of the channel. The T-matrix obeys following equation:

$$T^\alpha(p, p') = V^\alpha(p, p') + \int d\bar{p}\bar{p}^2 V^\alpha(p, \bar{p}) \frac{1}{E - E(\bar{p}) + i\epsilon} T^\alpha(\bar{p}, p'). \tag{4.3}$$

The equation can be solved by the matrix inversion or K-matrix method. The numerical calculation is performed by the standard integral method. The on-shell T-matrix is related

with the phase shift. Below the inelastic threshold it is expressed as

$$\mathrm{e}^{i\delta_\alpha}\sin\delta_\alpha = -\pi\rho T^\alpha(p_0,p_0), \tag{4.4}$$

$$\rho = p^2\left(\frac{\partial E(p)}{\partial p}\right)^{-1}\Bigg|_{p=p_0}, \tag{4.5}$$

where p_0 is on shell momentum which satisfy $E = E_\alpha(p_0)$. The wave function is given as

$$\chi^{(+)}_\alpha(p) \;=\; \frac{\delta(p-p_0)}{p^2} + \frac{1}{E - E_\alpha(p) + i\epsilon}T^\alpha(p,p_0). \tag{4.6}$$

For completeness, the configuration space wave function is given simply by the Fourier-Bessel transformation.

$$\chi^{(+)}_\alpha(r) = \int_0^\infty dp p^2 j_{\ell_\alpha}(pr)\chi^{(+)}_\alpha(p). \tag{4.7}$$

The potential V_{YN}, which we used, is the latest Nijmegen Soft Core potential 97 (NSC97). It is based on the standard SU(3) boson-exchange potential with inclusion of some explicit SU(3) breaking terms as, 1) physical masses for the baryons and mesons, and 2) Λ and Σ^0 mixing. They studied six parameter sets, all of which can describe the YN scattering well. Different parameter sets have different magnetic couplings of vector meson, $F/(F+D)$. Of all parameter sets, we adopt model F, since it reproduces the hypertriton binding energy. To be consistent with this YN potential, we also adopt the Nijmegen NN potential among the various available NN potentials. It includes breaking of charge independence, due to inclusion of physical masses for the baryons and mesons. As a result, their potential predicts the isovector np phase parameters smaller than those of pp phase parameters.

4.2 Total cross section

At first, we discuss the total cross section. It is expressed as

$$\sigma^{\mathrm{tot}} = \pi N \sum_{\ell\ell' SS' J}(2J+1)\Big|\langle((\ell' S')J;p_f|T|(\ell S)J;p_i\rangle\Big|^2. \tag{4.8}$$

As we expected, the distortion effects is extremely large. In Fig. 4, the effects of the final state YN interaction (FSI) by NSC model-f and the initial state NN interaction(ISI) are shown.

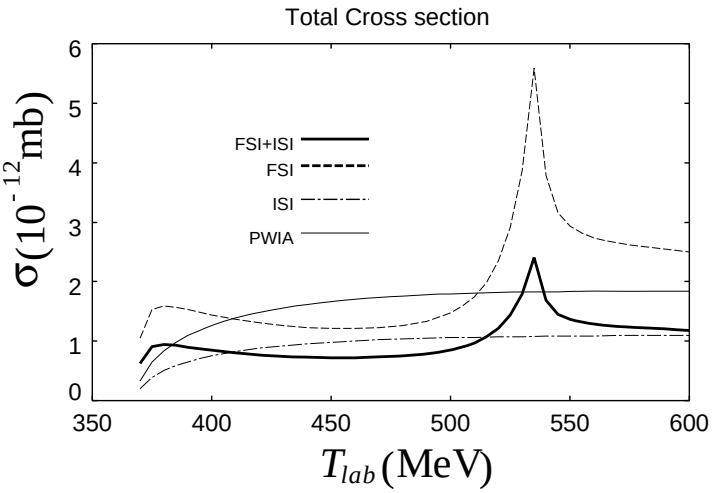

Figure 4: Total cross section of $p + n \to p + \Lambda$ reaction in the pion-exchange model. The thin solid line is calculated with plane waves. The dash-dotted line includes final state interaction, while the dashed line initial state interaction. The thick solid line is full calculation including the both distortion. NSC model-f is used for the final state interaction.

The ISI reduces the cross section by a factor 2 in the energy region we have studied, mainly due to the repulsive NN interaction at short range. On the other hand, FSI increases the total cross section near the threshold. Near the threshold energy, the final S-wave is dominant and attractive part of the YN interaction enhances the wave function as shown in Fig. 5. Around threshold region of ΣN production, the total cross section depends on the incident energy strongly due to the FSI. Inclusion of both the FSI and ISI gives total cross section of the order of $10^{-39}\mathrm{cm}^2$.

Before exploring the origin of the peak near the Σ threshold, we shall look around the contribution of each partial waves. Fig. 6 shows convergence of the total cross section with respect to the final orbital angular momentum. As expected, in the low energy region up to 400MeV, the S-wave, especially ${}^3S_1$, final state is important. But it should be noticed that this naive expectation may not apply to the polarization asymmetries, since the interference term plays an important role. As the incident energy increases up to the ΣN threshold, the D-wave, especially ${}^3D_1$, becomes important as shown in Fig. 6. Although we calculated partial waves

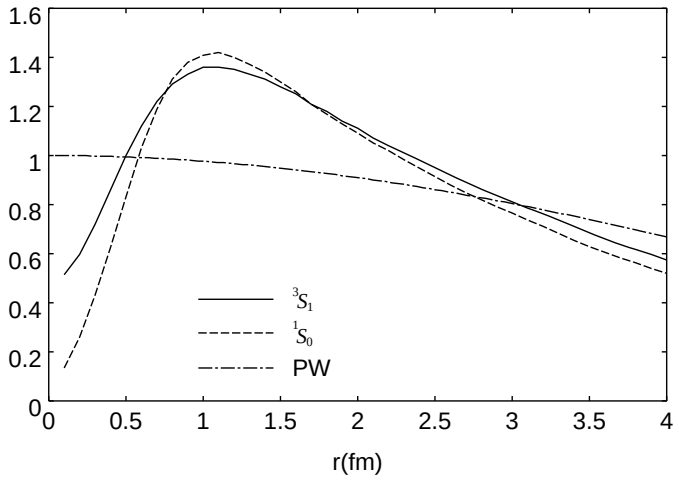

Figure 5: The ΛN wave function in the configuration space at $T_{lab} = 380$MeV. $^3S_1$ and $^1S_0$ ΛN wave function are shown in solid and dashed line, which are compared with plane wave in dash-dot-line.

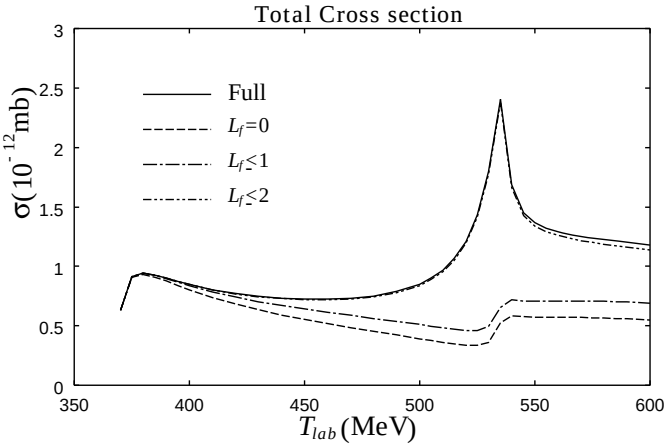

Figure 6: Total cross section of $p + n \to p + \Lambda$ reaction in the pion-exchange model. Maximum orbital angular momentum (L_f) of final state for dashed, dash-dotted and dash-two-dotted lines are S, P, and D-wave, respectively. Solid line include partial waves up to $L_f = 6$.

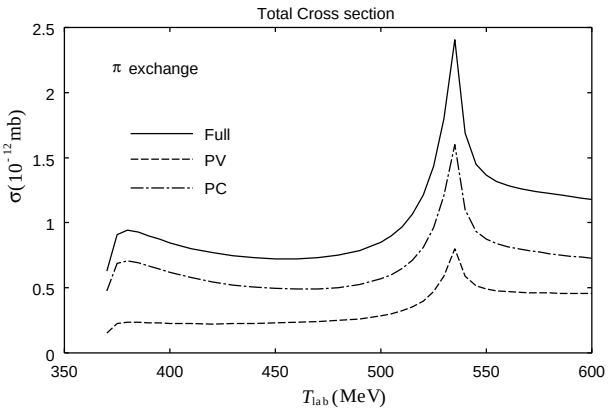

Figure 7: Contribution of parity-violating and parity-conserving amplitudes to the total cross section with pion-exchange potential. Dashed line includes parity-violating amplitude only while dash-dotted line includes parity-conserving one. Solid line shows a results including both of them.

up to $J = 6$, we found $J \leq 3$ is sufficient to describe the behavior of the total cross section of the $p + n \to p + \Lambda$ reaction in this energy region. To see which state contributes to this reaction, we summarize the matrix elements in the energy region of the first and second peaks in the tables 4 and 5.

From table 4, one can find the ${}^3S_1$ matrix element for YN plays dominant role. Nevertheless, the ${}^1S_0$ components are not negligible. For the second peak region, matrix elements between the final ${}^3D_1$ and each of the initial ${}^3D_1$, ${}^1P_1$ and ${}^3S_1$ are important. It is the feature of the NSC potential that causes strong $N\Sigma({}^3S_1)$ -$N\Lambda({}^3S_1 - {}^3D_1)$ mixing. As a result, the overlap integral is enhanced. It is worth while noticing that transitions from the ${}^3D_1$ and ${}^3S_1$ are caused by the parity-conserving interaction, while the transition from the ${}^1P_1$ is caused by parity-violating one.

In the pion-exchange potential, the parity-violating coupling constant, A_π, is about 7 times smaller than parity-conserving one, B_π, while their contributions to the total cross section are comparable with each other, as shown in Fig. 7. This is because $(\boldsymbol{p}/m)$ in the PC term is large.

We found that the initial $T = 0$ NN system gives dominant contribution to the cross

$^{J=0}_{F\backslash I}$	$^1S_0$	$^3P_0$
$^1S_0$	$\overset{a}{-16.17}$	$\overset{b}{38.31}$
$^3P_0$	0.02	3.42

$^{J=1}_{F\backslash I}$	$^1P_1$	$^3S_1$	$^3P_1$	$^3D_1$
$^1P_1$	0.85	3.31	0.19	-5.82
$^3S_1$	$\overset{e}{71.79}$	$\overset{c}{100.00}$	$\overset{f}{28.18}$	$\overset{d}{-116.72}$
$^3P_1$	0.71	0.89	-1.35	-1.67
$^3D_1$	-0.12	-0.75	-0.47	-0.06

$^{J=2}_{F\backslash I}$	$^1D_2$	$^3P_2$	$^3D_2$	$^3F_2$
$^3P_2$	-2.65	1.98	-8.80	5.08

(%)

Table 4: The relative ratio of the relevant matrix elements of pion-exchange potential for the $p + n \to p + \Lambda$ with initial kinetic energy at 380MeV.

$^{J=0}_{F\backslash I}$	$^1S_0$	$^3P_0$
$^1S_0$	$\overset{a}{-10.25}$	$\overset{b}{21.98}$
$^3P_0$	-0.08	12.34

$^{J=1}_{F\backslash I}$	$^1P_1$	$^3S_1$	$^3P_1$	$^3D_1$
$^1P_1$	9.17	15.44	0.87	-27.71
$^3S_1$	$\overset{e}{22.53}$	$\overset{c}{100.00}$	$\overset{f}{22.05}$	$\overset{d}{-26.82}$
$^3P_1$	4.15	5.87	-5.33	-6.81
$^3D_1$	182.06	-65.74	-14.63	-262.79

$^{J=2}_{F\backslash I}$	$^1D_2$	$^3P_2$	$^3D_2$	$^3F_2$
$^1D_2$	-0.57	3.13	-6.47	7.43
$^3P_2$	-14.26	11.10	-45.91	25.33
$^3D_2$	-2.26	-2.04	26.19	7.20
$^3F_2$	-1.01	-0.14	1.08	2.14

(%)

Table 5: The relative ratio of the relevant matrix elements of pion-exchange potential for the $p + n \to p + \Lambda$ with initial kinetic energy at 535MeV

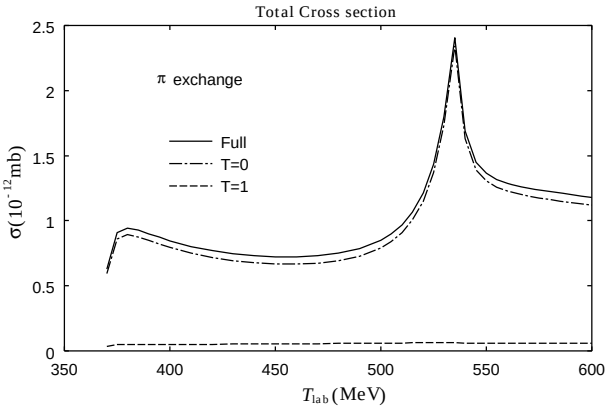

Figure 8: Contribution of each pn isospin state to the total cross section with pion-exchange potential. Dashed line shows contribution from the $T = 1$ initial pn pair, while dash-dotted line shows contribution from the $T = 0$ states. Solid line includes both contributions.

section as shown in Fig. 8. This is because contributions of the charged pion-exchange and neutral pion-exchange mechanism are destructive with each other for $T = 1$ pn system, while constructive for $T = 0$ pn system.

Fig. 9 shows the dependence of various parameter set in NSC97 model (a-f). They differ about 30% at the energy of the first peak, due to the strength of spin-spin term. Hereafter we fix the YN potential to NSC97 model-F.

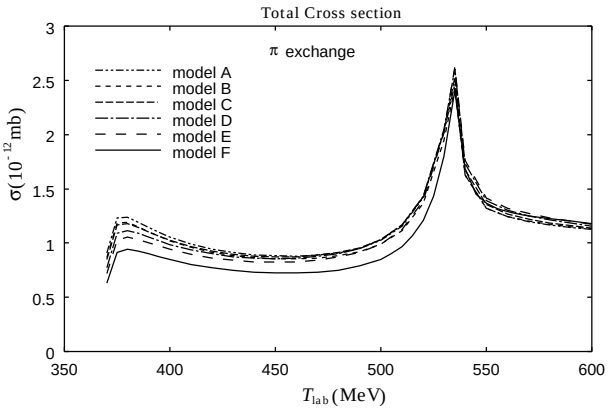

Figure 9: Total cross section with pion-exchange potential with various NSC97 interaction

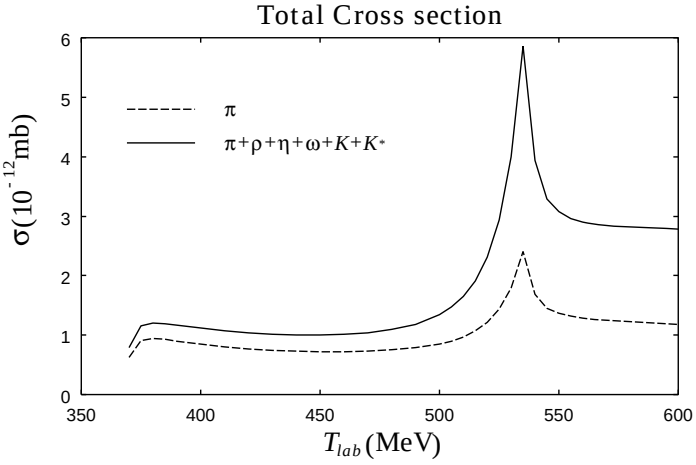

Figure 10: Contribution of various mesons to the total cross section. Dashed line shows pion-exchange only, while solid line includes all six meson-exchange mechanism.

As shown in Fig. 10, inclusion of other mesons enhances the total cross section about 30% near the threshold, and 250% near the ΣN threshold. Nevertheless, as shown in Fig. 11, the pion-exchange potential gives the most important contribution. The enhancement comes from the additive contribution of meson-exchange potentials.

Separating contributions of PV and PC term from each other, we find drastic changes of the cross section from only the pion-exchange , as shown in Fig. 12. The PV term accounts for the main part of the cross section. Contributions of each mesons for PV and PC amplitude are shown in Figs. (13-a) and (13-b). While there exist strong cancellations between the various meson-exchange mechanisms in the PC term, they contribute constructively to the PV term. This effect can be seen in the polarization observables.

It is worth while noticing that destructive or constructive interference of pseudoscalar and vector meson holds also for the inverse reaction $\Lambda N \to NN$. Our results disagree with those in Ref.[33], which states that the parity violating term in the vector meson exchange potential has opposite sign to ours. We cannot reproduce their sign even if we use the same Hamiltonian for both the strong and weak interactions. The transition potential in Ref. [29, 32] have the same relative sign between π and ρ as ours. But there are many literatures which take incorrect

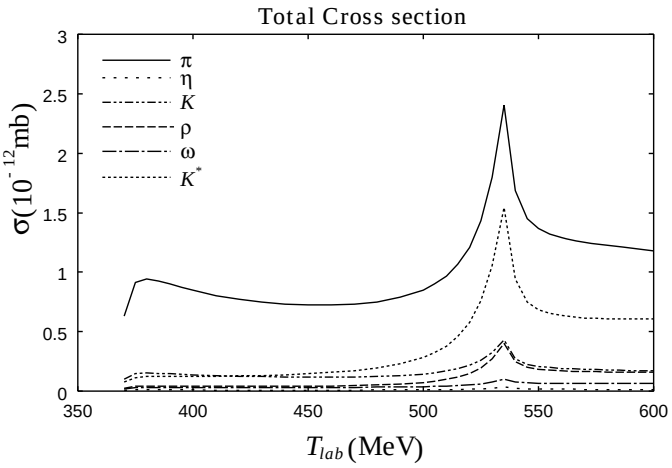

Figure 11: Contribution of the each meson exchange potential to the total cross section

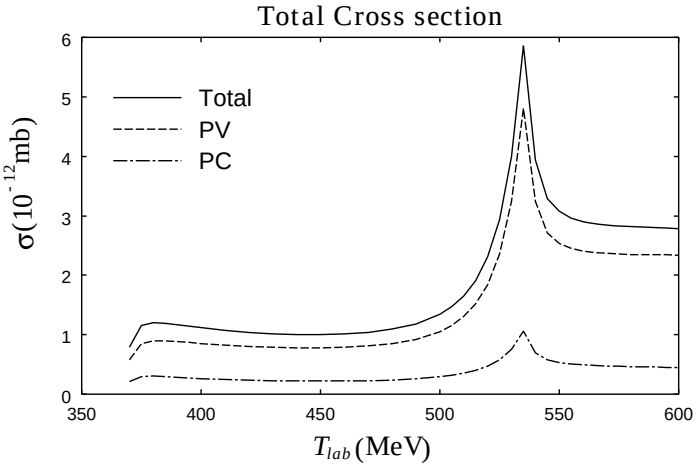

Figure 12: Contribution of parity-violating and parity-conserving amplitudes to the total cross section with full meson exchange mechanism. The dashed line shows the contribution from the PV term, while the dash-dotted line from PC term.

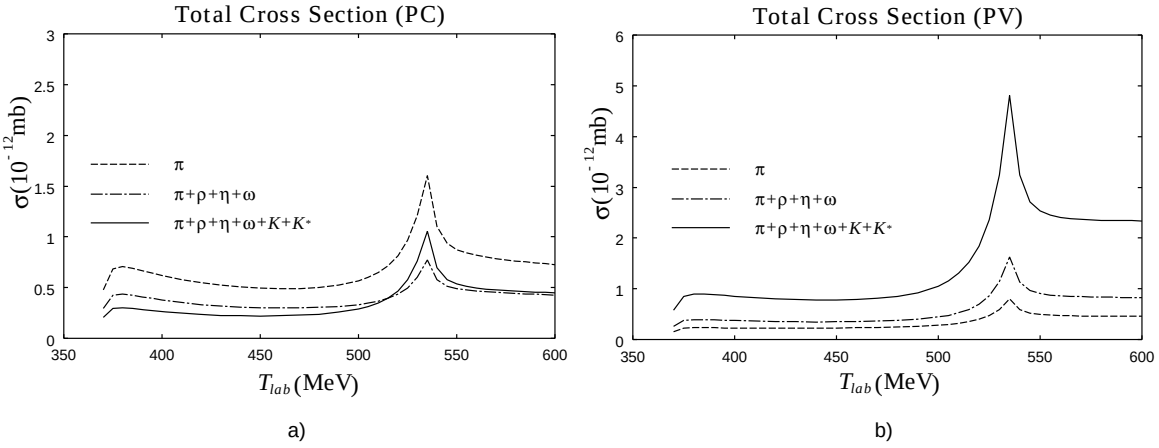

Figure 13: Contribution of meson exchange mechanism for PV and PC amplitude. Dashed line shows the pion-exchange contribution, while dash-dotted line shows contribution of the non-strangeness meson . Solid line includes all meson-exchange mechanism.

signs. Changing the relative sign of parity violating term between pseudoscalar and vector meson-exchange potential does change the results of total cross section drastically, as shown in Fig. 14. If we flip the sign of the PV term in the vector meson-exchange potential, the strong enhancement observed in our original choice of phase, does not occur, and the total cross section is reduced by about a factor 4 around the ΣN threshold.

4.3 Polarization observable

In this section we present our results on polarization observables. P and T transformation properties of each polarization observables are summarized in the table 1 in section 2. We can discuss general interference structure of polarization observable. In our model of boson exchange weak BB interaction, we took only local operators. In the coordinate space the general form of the parity conserving part of V_W is written, apart from of the isospin structure, as

$$V_W^{PC} = f_c(r) + f_\sigma(r)\boldsymbol{\sigma}_1 \cdot \boldsymbol{\sigma}_2 + f_T S_{12} \tag{4.9}$$

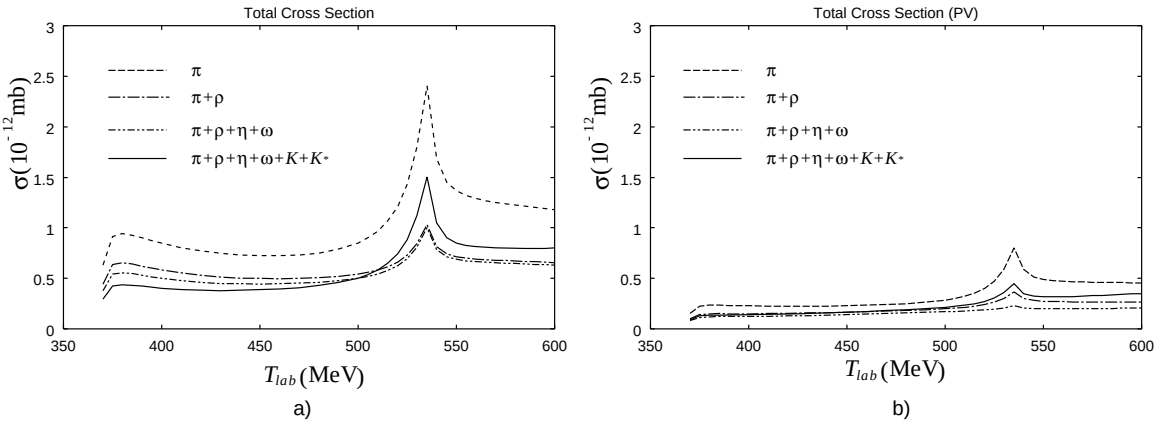

Figure 14: Total cross section with opposite sign of ϵ. a) Contribution of each meson exchange mechanism to the total cross section. b) Contribution of each meson exchange mechanism to PV amplitude, which is compared with Fig. 13-b.

and, parity-violate part, as

$$V_W^{PV} = \boldsymbol{\sigma}_1 \cdot \hat{\boldsymbol{r}} f_{\sigma 1}(r) + \boldsymbol{\sigma}_2 \cdot \hat{\boldsymbol{r}} f_{\sigma 2}(r) + i\boldsymbol{\sigma}_1 \times \boldsymbol{\sigma}_2 \cdot \hat{\boldsymbol{r}} f_{\sigma\times}(r) \tag{4.10}$$

Here the $f_{\sigma 1,2}$ terms are due to pseudoscalar meson-exchange potential, and vector meson-exchange potential has a $f_{\sigma\times}$ term only. Then, we have four types of matrix elements of V_W^{PC} as

$$\langle {}^3E_J|V_W^{PC}|{}^3E_J\rangle, \tag{4.11}$$

$$\langle {}^1O_J|V_W^{PC}|{}^1O_J\rangle, \tag{4.12}$$

$$\langle {}^1E_J|V_W^{PC}|{}^1E_J\rangle, \tag{4.13}$$

$$\langle {}^3O_J|V_W^{PC}|{}^3O_J\rangle. \tag{4.14}$$

Here we denote the two baryon state as ${}^{2S+1}L_J$, where L is even or odd for initial NN and final YN states.

The matrix elements of V_W^{PV} are given by

$$\langle {}^1O_J|V_W^{PV}|{}^3E_J\rangle \tag{4.15}$$

$$\langle {}^1E_J|V_W^{PV}|{}^3O_J\rangle \tag{4.16}$$

$$\langle {}^3O_J|V_W^{PV}|{}^1E_J\rangle \tag{4.17}$$

$$\langle {}^3E_J|V_W^{PV}|{}^1O_J\rangle \tag{4.18}$$

$$\langle {}^3O_J|V_W^{PV}|{}^3E_J\rangle \tag{4.19}$$

$$\langle {}^3E_J|V_W^{PV}|{}^3O_J\rangle \tag{4.20}$$

Matrix elements of V_W^{PV} always accompany the spin-flip of baryons except for (4.19) and (4.20), to which only pseudoscalar meson exchange process contributes. It is noticed that there are no matrix elements between spin-singlet states because of the spin structure of V_W^{PV}.

Near the threshold energy of Λ production, ${}^{2S+1}E_J$ final state is dominant. The final ${}^3S_1$ states are lead by the initial NN states with $T = 0$ for both PV and PC case, while the ${}^1S_0$ final YN state is lead by the NN states with $T = 1$.

On the angular integrated single polarizations $\bar{A}_p$ and $\bar{A}_\Lambda$, we can proceed furthermore. To obtain $\bar{A}_\Lambda$, we have to average over the initial spin states of the NN system, so that there appear no interference terms between spin-triplet and singlet NN states. Since we integrate over the final angular distribution and $\bar{A}_\Lambda$ is parity-violating observable, $\bar{A}_\Lambda$ is given by the interference of $T = 0$ and $T = 1$ initial states. Therefore, by observing $\bar{A}_\Lambda$, one can test relatively small $T = 0$ amplitude.

On the contrary, $\bar{A}_p$ includes no interference terms between spin-triplet and singlet YN states. In this case there are no interference term of $T = 0$ and $T = 1$ initial NN states. However, $\bar{A}_p$ includes the interference of $S_{NN} = 1$ and $S_{NN} = 0$ amplitude. Therefore, near threshold we may test the interference term of mainly ${}^3E$ and ${}^1O$ initial states.

In what follows, we will show the mechanism of polarization using the simple plane wave approximation. Then we show the results of the energy dependence of single and double polarization, and finally the angular distribution of observables.

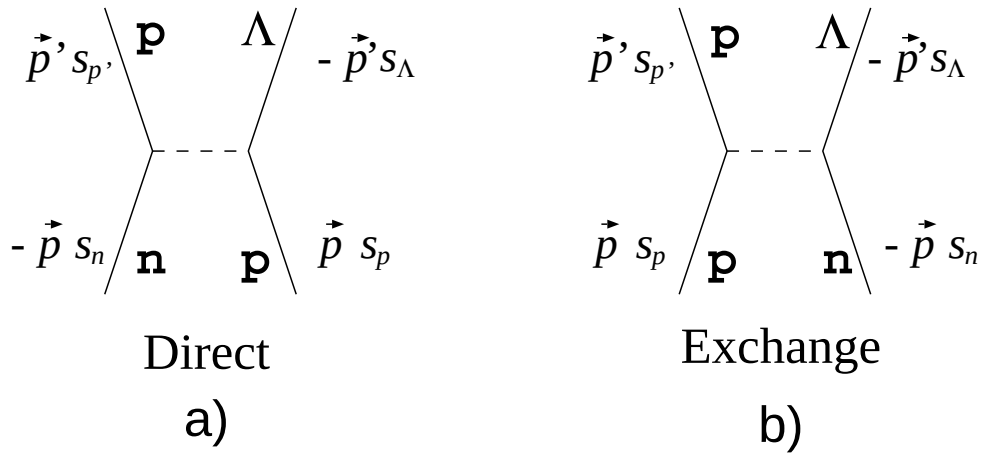

Figure 15: Schematic representation of $p + n \to p + \Lambda$ reaction on particle base.

4.3.1 Mechanism of polarization in $p + n \to p + \Lambda$ reaction

Although we wrote the V_W by adopting isospin formalism with spurion for Λ, it is convenient to work in particle bases to discuss polarization mechanism. Near the threshold energy of Λ production, we can neglect momentum of final state. The matrix elements of V_W in plane wave is given by the two terms. The one is 'direct' process when initial proton is converted into Λ as shown in Fig. 15-a. The other is 'exchange' process where neutron is converted into Λ shown in Fig.15-b.

In our model of V_W, direct part is given as

$$V_W^D = V_W^{D,PC} + V_W^{D,PV} \tag{4.21}$$

and

$$V_W^{D,PC} = \left[f_c^D + \boldsymbol{\sigma}_1 \cdot \boldsymbol{\sigma}_2 f_\sigma^D + (\boldsymbol{\sigma}_1 \cdot \hat{\boldsymbol{p}})(\boldsymbol{\sigma}_2 \cdot \hat{\boldsymbol{p}}) f_T^D\right]_{(s'_p, s_\Lambda; s_n, s_p)} , \tag{4.22}$$

$$V_W^{D,PV} = \left[\boldsymbol{\sigma}_1 \cdot \hat{\boldsymbol{p}} f_{\sigma 1}^D + \boldsymbol{\sigma}_2 \cdot \hat{\boldsymbol{p}} f_{\sigma 2}^D + i\boldsymbol{\sigma}_1 \times \boldsymbol{\sigma}_2 \cdot \hat{\boldsymbol{p}} f_{\sigma\times}^D\right]_{(s'_p, s_\Lambda; s_n, s_p)} . \tag{4.23}$$

Here spin matrix element should be taken as

$$\mathcal{O}_{(s'_p, s_\Lambda; s_n, s_p)} \equiv \langle s'_p | \mathcal{O}_1 | s_n \rangle \langle s_\Lambda | \mathcal{O}_2 | s_p \rangle . \tag{4.24}$$

The exchange process is given by the same formula but the spin index $(s'_p, s_\Lambda; s_n, s_p)$ should be replaced by $(s'_p, s_\Lambda; s_p, s_n)$.

For the pion-exchange model is given by

$$\begin{aligned} V_W^D &= V_W^{D,PC} + V_W^{D,PV} && (4.25)\\ &= \bar{N}[2(\boldsymbol{\sigma}_1 \cdot \hat{\boldsymbol{p}})(1 - \lambda \boldsymbol{\sigma}_2 \cdot \hat{\boldsymbol{p}})] \ , && (4.26)\\ V_W^E &= V_W^{E,PC} + V_W^{E,PV} && (4.27)\\ &= \bar{N}[-(\boldsymbol{\sigma}_1 \cdot \hat{\boldsymbol{p}})(1 + \lambda \boldsymbol{\sigma}_2 \cdot \hat{\boldsymbol{p}})] \ , && (4.28) \end{aligned}$$

where N and λ defined as

$$\begin{aligned} \bar{N} &= -\frac{G_F m_\pi^2}{(2\pi)^3 \omega_\pi^2} \Big(\frac{g_{NN\pi}}{2m_N} \Big) A_\pi |\boldsymbol{p}| \ , && (4.29)\\ \lambda &= \frac{B_\pi}{A_\pi} \frac{|\boldsymbol{p}|}{2m_N} \ . && (4.30) \end{aligned}$$

'Direct' process is given by the charged pion exchange mechanism and the 'exchange' process is given by the neutral pion exchange mechanism. Magnitude of 'direct' process is 2 times larger than the 'exchange' process because of $\Delta I = \frac{1}{2}$ rule.

Therefore in this model we obtain

$$\begin{aligned} f_T^D &= -2\lambda \bar{N}, \quad f_T^E = -\lambda \bar{N}, \\ f_{\sigma 1}^D &= 2\bar{N}, \quad f_{\sigma 1}^E = -\bar{N}, \\ f_\sigma^D &= 2\lambda' \bar{N}, \quad f_\sigma^E = \lambda' \bar{N}. && (4.31) \end{aligned}$$

The other f's vanish. Here λ' is introduced to estimate the short range correlation to drop the δ-function type potential, and given as

$$\lambda' = \frac{\lambda}{3} \Big(1 + \frac{m_\pi^2}{|\boldsymbol{p}|^2} \Big). \qquad (4.32)$$

To switch off the short range correlation, just set $\lambda' = 0$.

Now in the case of free Λ decay into a pion and a nucleon, the asymmetry parameter A_Λ and A_p are given as

$$\tilde{A}_N = \tilde{A}_\Lambda = \frac{-2\lambda}{\lambda^2 + 1} > 0 \ . \qquad (4.33)$$

They have the same magnitude and positive value.

We take the quantization axis as the direction of the incident proton momentum. The polarization $\bar{A}_p$ and $\bar{A}_\Lambda$ are easily calculated. In the 'direct' process, spin of proton and Λ is connected by the weak vertex which is same as free Λ decay. Therefore if we take only direct term, we obtain

$$A_p^D = A_\Lambda^D = \tilde{A}_\Lambda, \tag{4.34}$$

while the exchange process gives

$$A_\Lambda^E = -\tilde{A}_\Lambda, \quad A_p^E = 0. \tag{4.35}$$

In $p + n \to p + \Lambda$ reaction, of course the two process interfere and the situation becomes a little complicated, but easily we obtain

$$A_p = \frac{-8\lambda}{7\lambda^2 + 3 + 9\lambda'^2 - 6\lambda\lambda'} \sim 0.72(0.64) , \tag{4.36}$$

$$A_\Lambda = \frac{-6\lambda + 6\lambda'}{7\lambda^2 + 3 + 9\lambda'^2 - 6\lambda\lambda'} \sim 0.34(0.48) , \tag{4.37}$$

$$A_p > \frac{4}{3} A_\Lambda . \tag{4.38}$$

We also show the numerical value at the Λ production threshold where $|\boldsymbol{p}| \sim 417$MeV/c. The values with parenthesis are results without short range correlation. $\bar{A}_\Lambda$ decreases about 30%, while $\bar{A}_p$ is not affected much. Proton asymmetry is larger than Λ asymmetry and they are both positive. When we include another meson, spin, isospin, strangeness exchange processes modify the polarization observables in a different way from the free Λ decay.

In the case of double polarization, we can do the same calculation, and the results are

$$A_{L1} = \frac{-14\lambda + 6\lambda'}{13\lambda^2 + 5 + 9\lambda'^2 - 18\lambda\lambda'} \sim 0.80(0.61) ,$$

$$A_{L2} = \frac{-2\lambda - 6\lambda'}{\lambda^2 + 1 + 9\lambda'^2 + 6\lambda\lambda'} \sim 0.57(0.92) ,$$

$$A_{L3} = \frac{6\lambda^2 - 6\lambda + 2 - 12\lambda\lambda' + 6\lambda'}{7\lambda^2 - 8\lambda + 3 + 9\lambda'^2 - 6\lambda\lambda'} \sim 0.39(0.80) ,$$

$$A_{L4} = \frac{-6\lambda^2 - 6\lambda - 2 + 12\lambda\lambda' + 6\lambda'}{7\lambda^2 + 8\lambda + 3 + 9\lambda'^2 - 6\lambda\lambda'} \sim 0.035(-0.96) ,$$

$$A_{L5} = \frac{6\lambda^2 - 8\lambda + 2 - 12\lambda\lambda'}{7\lambda^2 - 6\lambda + 3 + 9\lambda'^2 - 6\lambda\lambda' + 6\lambda'} \sim 0.79(0.99) ,$$
$$A_{L6} = \frac{-6\lambda^2 - 8\lambda - 2 + 12\lambda\lambda'}{7\lambda^2 + 6\lambda + 3 + 9\lambda'^2 - 6\lambda\lambda' - 6\lambda'} \sim 0.59(-0.36) . \quad (4.39)$$

One can show A_{L4} and A_{L6} are sensitive to the short range correlation.

As a result, we expect

$$A_{L1} \sim A_{L5} > A_{L6} \sim A_{L2} > A_{L3} > A_{L4} \sim 0 \quad (4.40)$$

near the Λ production threshold.

For the transverse double polarization, this estimation gives

$$A_{T1} = \frac{-12\lambda^2 + 4 + 12\lambda\lambda'}{14\lambda^2 + 6 + 18\lambda'^2 - 12\lambda\lambda'} \sim -0.40(-0.62) . \quad (4.41)$$

Since we do not include time reversal violated interaction, PWIA calculation of A_{T2} leads to zero.

This simple estimation gives surprisingly a good agreement with our detailed numerical result except for transverse polarization.

4.3.2 Single polarization

The asymmetry $\bar{A}_p$ is obtained by measuring the difference of the integrated cross section using proton beam with the positive and negative helicity state. Similarly $\bar{A}_\Lambda$ is obtained by measuring the polarization of Λ in the direction of proton beam.

The energy dependence of $\bar{A}_p$ and $\bar{A}_\Lambda$ is shown in the Fig. 16 by using pion exchange model of V_W. Initial NN state interaction enhances the $\bar{A}_p$ in all energy region, while it reduces $\bar{A}_\Lambda$. The final state interaction is significant near the energy region of Σ production threshold. As we discussed in the previous section, both polarizations are positive and $\bar{A}_p$ is larger than $\bar{A}_\Lambda$ At the threshold $\bar{A}_p$ is around 0.76 and $\bar{A}_\Lambda$ is 0.30 which is in a good agreement with the naive estimation.

The contribution of each partial wave of final ΛN is shown in Fig. 17. For both polarizations the S-wave final state dominates, while the D-wave final state becomes important near the Σ threshold.

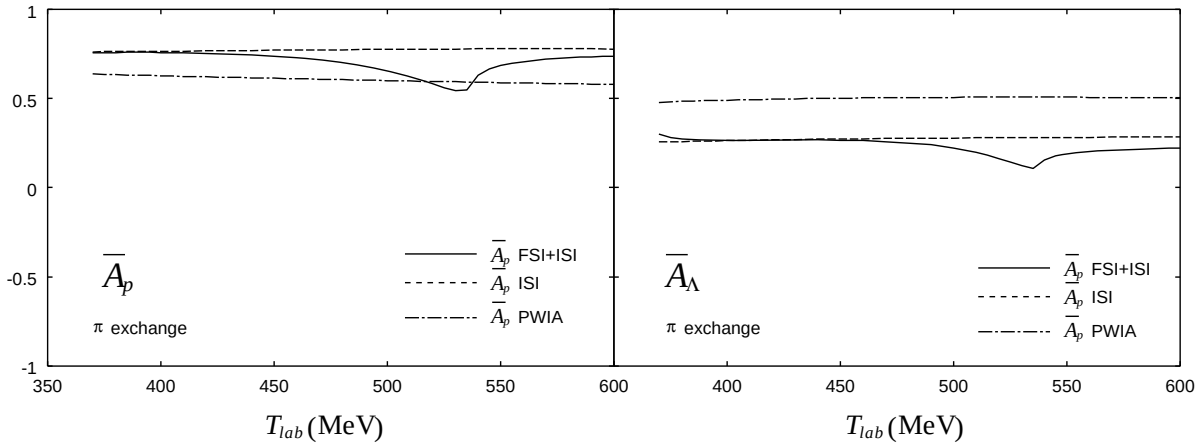

Figure 16: Effects of FSI and ISI to $\bar{A}_p$ and $\bar{A}_\Lambda$. The PWIA calculation is shown in dash-dotted line, while ISI is included in dashed-line. The solid line includes both FSI and ISI.

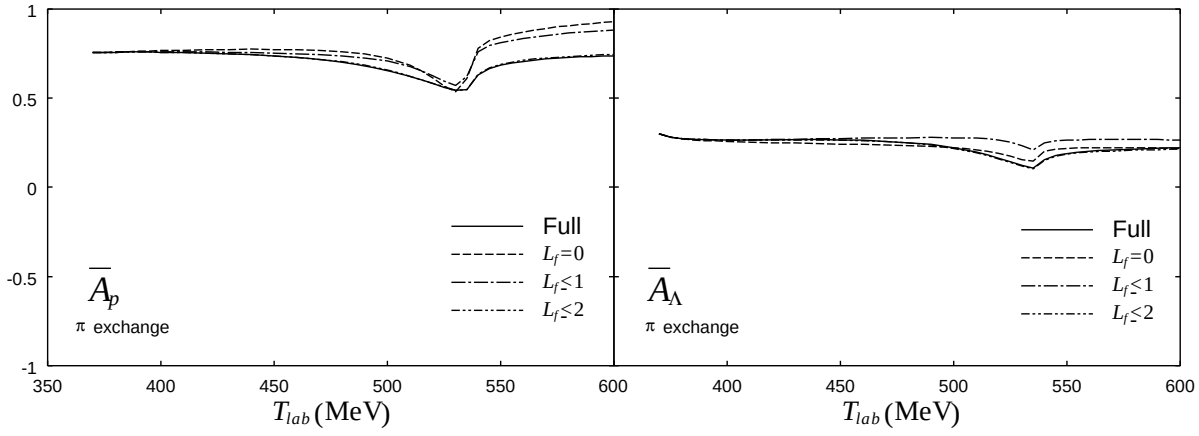

Figure 17: Convergence properties with respect to the final orbital angular momentum for $\bar{A}_p$ and $\bar{A}_\Lambda$

The contribution of the each meson-exchange weak BB interaction is shown in Fig. 18. Results including all meson-exchanges are shown by the solid line. The results are not very

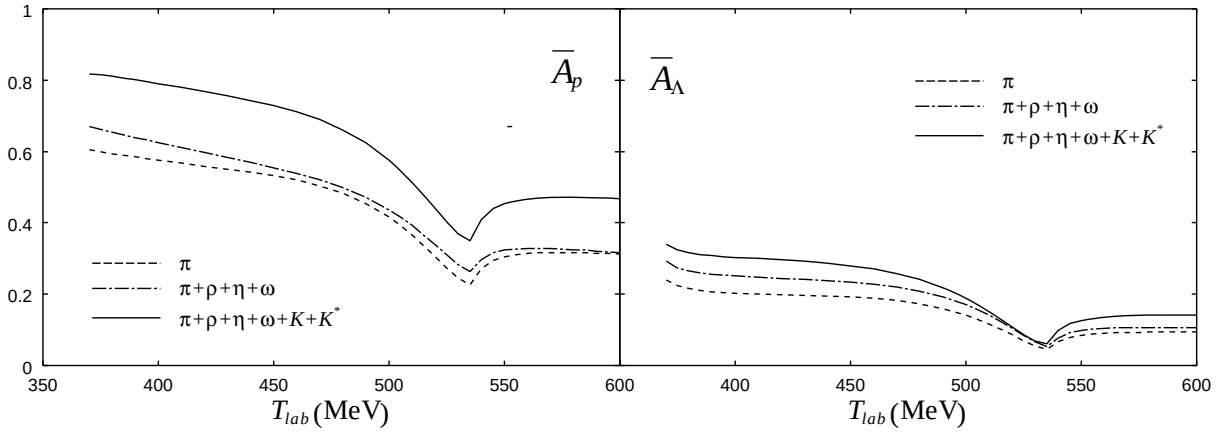

Figure 18: Contribution of each meson exchange mechanism to the $\bar{A}_p$ and $\bar{A}_\Lambda$. All meson exchange mechanism is included in sold line while the dash-dotted line includes non-strangeness ones. The dash line includes only pion-exchange mechanism.

different from those of only the pion-exchange mechanism in Fig. 16. They are both positive and $\bar{A}_p$ is larger than $\bar{A}_\Lambda$. Although the results with full meson-exchange model are similar to pion-exchange model, each contribution of mesons is different in $\bar{A}_p$ and $\bar{A}_\Lambda$. The strangeness exchange does give a large contribution to $\bar{A}_p$, while its effect is not so large for $\bar{A}_\Lambda$.

Even though the contribution of isoscalar NN state in the total cross section was negligible, the interference between $T = 0$ and $T = 1$ NN states give relatively large polarization $\bar{A}_\Lambda$ of about 0.4, which shows the $\bar{A}_\Lambda$ is useful quantity to test the ratio between $T = 0$ and $T = 1$ amplitudes. Since we already know the $^3S_1$ state is dominant in the final states at threshold, this is essentially given by the interference between the amplitudes with $NN\ ^3E$ to $YN\ ^3E$ and $NN\ ^3O$ to $YN\ E$.

Relatively large polarization of $\bar{A}_p$ was obtained for the case that the main contribution is the interference between the amplitudes with $NN\ ^3E$ to $YN\ ^3E$ and $NN\ O$ to $YN\ ^3E$.

In the matrix elements with $^3E_{\Lambda N}$–$^3O_{NN}$, most of the meson exchange mechanism contribute constructively in our model. The phase ambiguity between pseudoscalar and vector meson in the

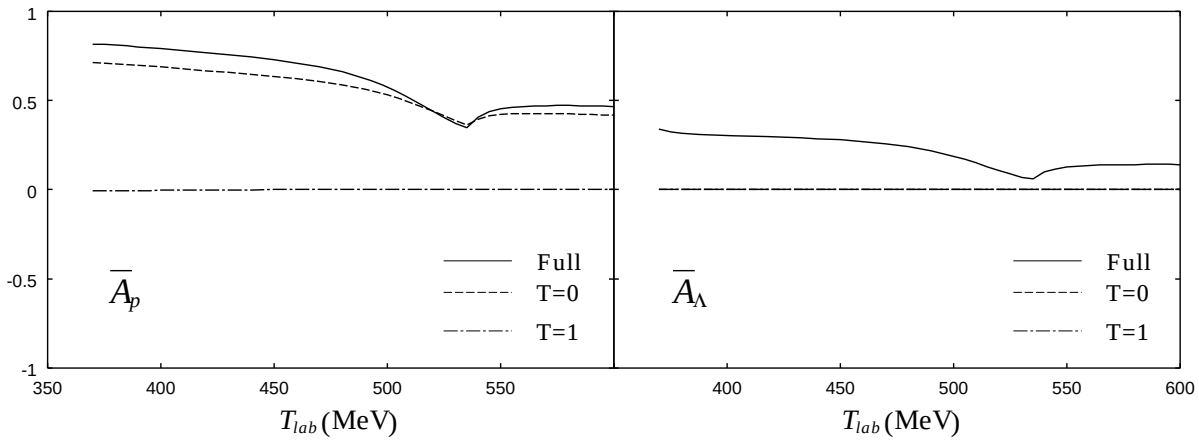

Figure 19: Isospin of initial pn system dependence of $\bar{A}_p$ and $\bar{A}_\Lambda$ with full meson exchange.

PV part of V_W affects this matrix element. As we can see in Fig.20, the results of $\bar{A}_p$ drastically change if we change the sign ϵ in V_W, while $\bar{A}_\Lambda$ is little affected. Therefore measuring of $\bar{A}_p$ will give us a clean answer to the question of the model of V_W.

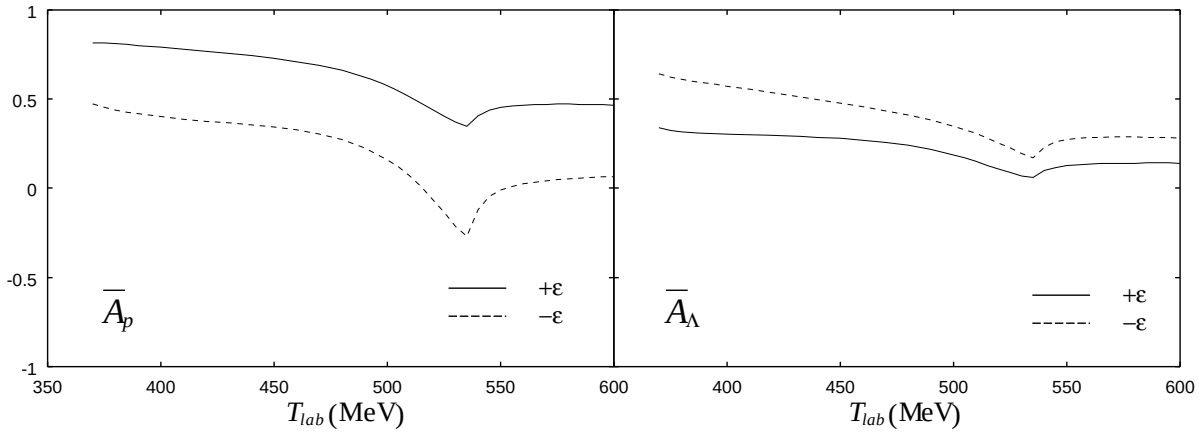

Figure 20: $\bar{A}_p$ and $\bar{A}_\Lambda$ with the change of the relative sign of parity violating term in the pseudoscalar and vector exchange potential.

4.3.3 Double polarization

There are four independent asymmetry parameters which are invariant under time reversal and one time-reversal violated observables. Among the four T-invariant quantities, two of them are $\bar{A}_p$ and $\bar{A}_\Lambda$ which can be obtained by the single polarization measurement. Therefore using double polarization, we can obtain two additional quantities. We have examined all six possible

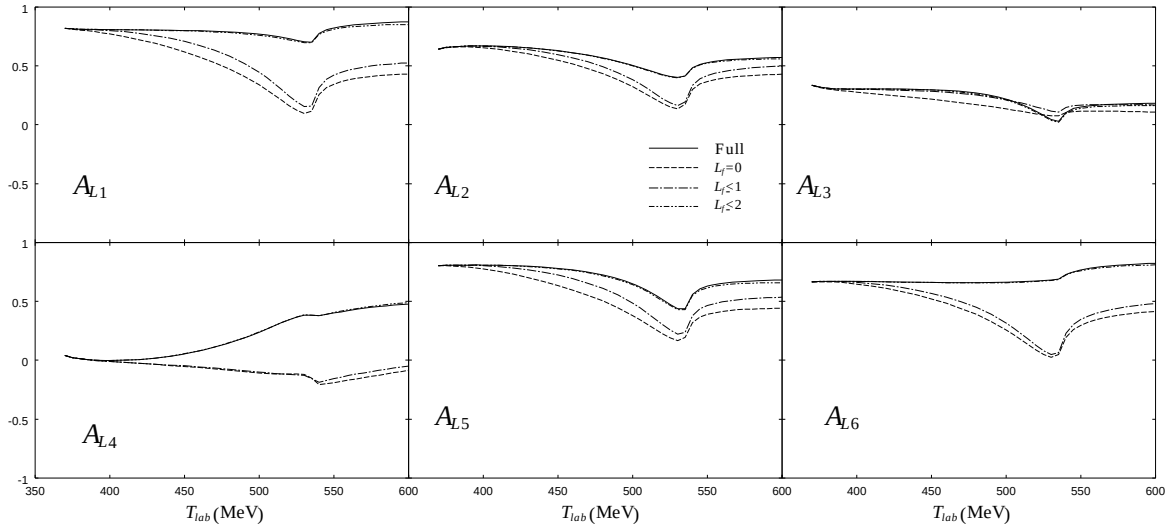

Figure 21: L_f dependence of $\bar{A}_{Li}$ with pion-exchange potential

longitudinal asymmetry observables. Longitudinal means all the spin is measured with respect to the incident momentum of proton. Fig. 21 shows the A_{Li} in the pion-exchange model of V_W. Near threshold energy region of Λ production the S-wave final state is sufficient but around Σ production energy, the D-wave final state becomes important. Asymmetry parameter A_{L4} changes sign including D-wave and is very sensitive to it.

Again the simple model discussed in previous section agrees with the DWIA full calculation. Near the threshold, the $\bar{A}_{Li}$s are

$$\begin{aligned} &\bar{A}_{L1} \sim 0.82 \ , \qquad \bar{A}_{L2} \sim 0.64 \ , \quad \bar{A}_{L3} \sim 0.33 \ , \\ &\bar{A}_{L4} \sim 0.04 \ , \qquad \bar{A}_{L5} \sim 0.80 \ , \quad \bar{A}_{L6} \sim 0.66 \ , \end{aligned} \tag{4.42}$$

so that the naive model with the short range correlation explain almost perfectly, which means

the observable $\bar{A}_{L4}$ and $\bar{A}_{L6}$ are very sensitive to the short range correlation.

As shown in Fig. 22, since the matrix elements with $T = 0$ dominates, A_{Li} are determined by the $T = 0$ initial NN state except $\bar{A}_{L3}$ and $\bar{A}_{L4}$ where interference between matrix elements of $T = 0$ and $T = 1$ states is essential. The results of A_{Li} including all the meson exchange

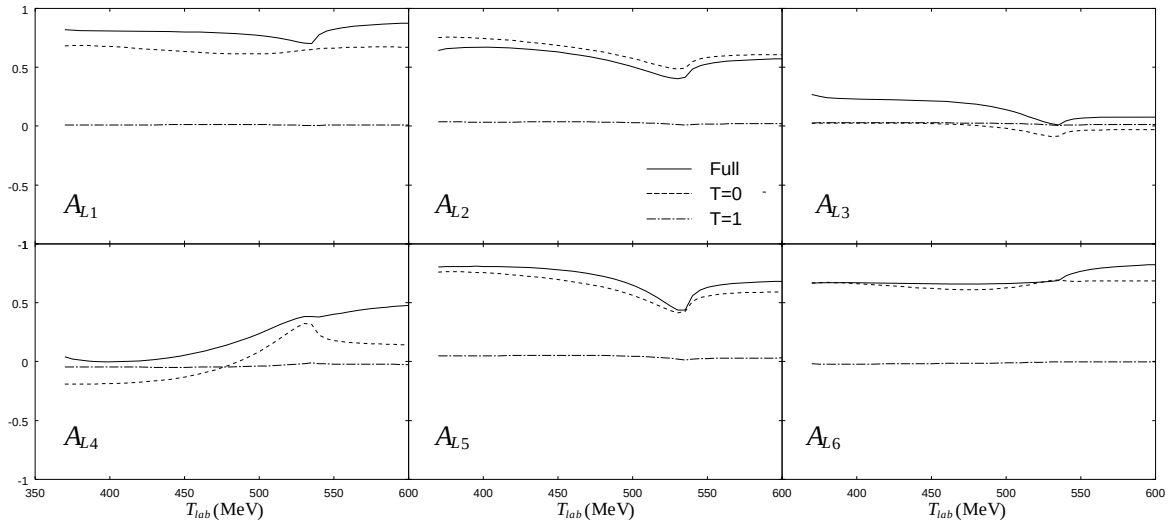

Figure 22: A_{Li} dependence on the initial pn isospin states with pion-exchange potential. The dashed and dash-dotted lines show the contribution from $T = 0$ and $T = 1$ NN states, respectively.

potential are given by the solid line in Fig. 23. Compared with pion-exchange, $\bar{A}_{L1}$, $\bar{A}_{L5}$ and $\bar{A}_{L6}$ are enhanced and have large value of the asymmetry parameter. $\bar{A}_{L2}$ and $\bar{A}_{L3}$ are affected relatively small. Again $\bar{A}_{L4}$ is very much modified if included are strange mesons, in particular K^*. A_{L4} may be an interesting quantity to determine the magnitude of strange meson exchange mechanism.

Like a single polarization asymmetry $\bar{A}_p$, double polarization asymmetries are sensitive to the relative phase of pseudoscalar and vector meson PV parts of V_W. As we can see in Fig. 24, all the asymmetries drastically change if we change the sign of ϵ in V_W. Especially, $\bar{A}_{L4}$, $\bar{A}_{L2}$ and $\bar{A}_{L6}$ change their signs.

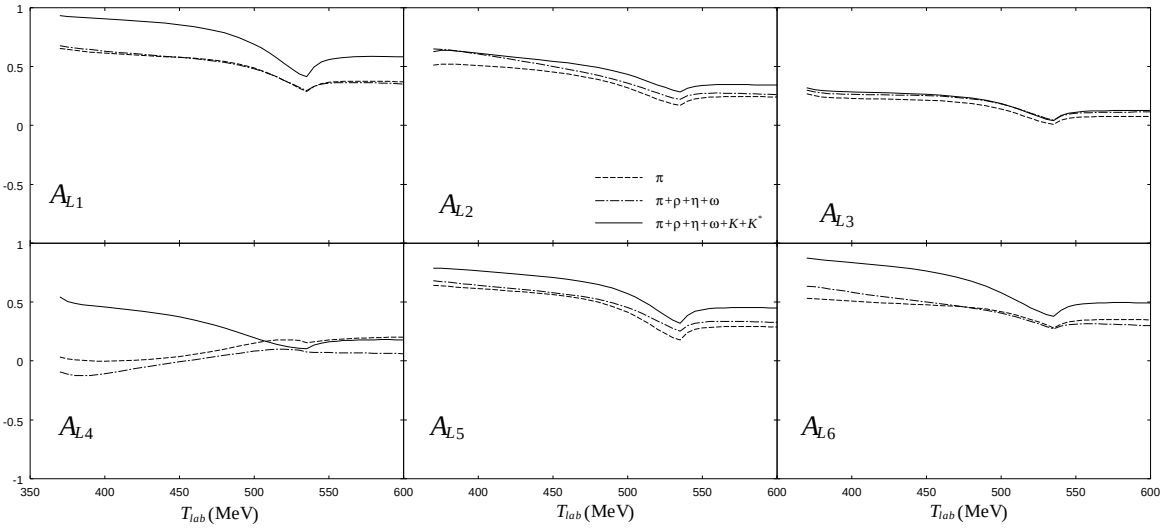

Figure 23: Dependence to the meson exchange mechanism on $\bar{A}_{Li}$. Solid line includes the all meson exchange mechanism, while the dash-dotted line include non-strangeness-exchange mechanism. The dash line includes only pion-exchange mechanism.

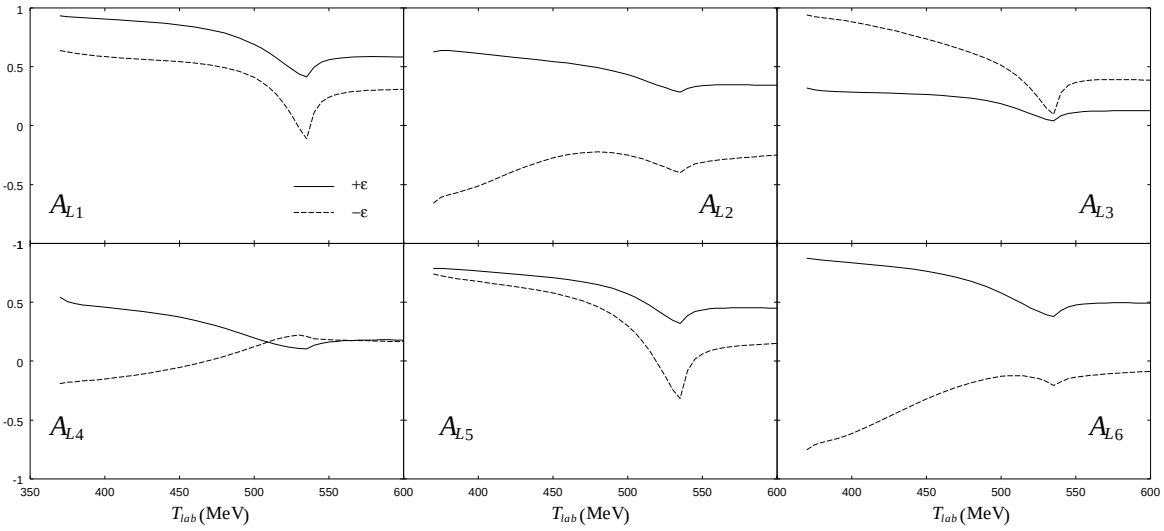

Figure 24: A_{Li}. See caption of Fig. 20

There is only one parity conserving observable, i.e., transverse polarization $\bar{A}_{T1}$. This quantity allows us to separate $\bar{A}^0_{p\Lambda}$ and $\bar{A}^2_{p\Lambda}$ along together with $\bar{A}_{Li}$ and shows interesting aspect of V_W. Since the quantity is parity conserved observable, no interferences between PC and PV of V_W appear in the total cross section nor the decay rate of hypernuclei. However, as shows in Fig. 25, PC and PV parts of V_W give opposite sign to $\bar{A}_{T1}$ and the relative magnitude of them can be measured by $\bar{A}_{T1}$. In Fig. 26 dotted line gives the contribution of pion-exchange

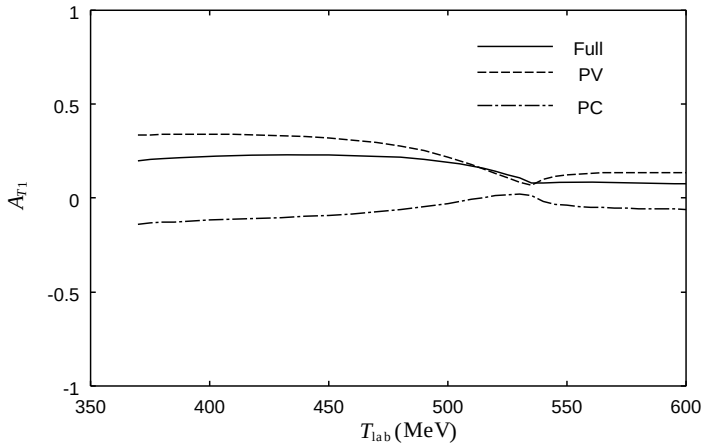

Figure 25: PC and PV contribution to A_{T1} Dashed line stands for PV contribution, while the dash-dotted for PC contribution.

mechanism, all non-strange meson exchange mechanisms are included in dashed line and finally mesons with strangeness are added in solid line. Here by including the meson with strangeness, $\bar{A}_{T1}$ is enhanced by about factor 2 around threshold energy of Λ production.

Finally we have estimated time-reversal and parity violating observable $\bar{A}_{T2}$ which is schematically expressed as

$$\langle \boldsymbol{J}_\Lambda \times \boldsymbol{J}_p \cdot \boldsymbol{p} \rangle \ . \tag{4.43}$$

Although our V_W is invariant under T, final and initial state interactions give non-vanishing $\bar{A}_{T2}$. Therefore our results will set limits on the order of magnitude where real $\not{T}$ effects could be observed. Although $\bar{A}_{T2}$ depend on the meson-exchange mechanism of V_W, as shown in

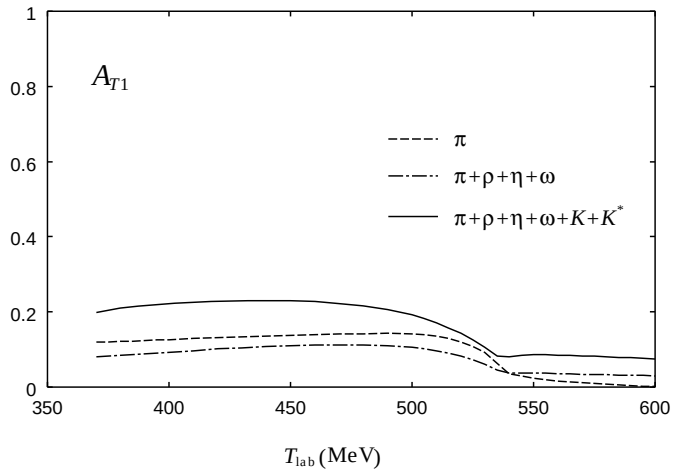

Figure 26: A_{T1}. Solid line shows the all meson exchange mechanism, while the dash-dotted line includes only non-strangeness ones. The dash line includes only pion-exchange mechanism.

Fig.27 order of magnitude of $\bar{A}_{T2}$ is at most 0.1. It will be very hard to detect genuine $\not{T}$ if they are less than 10% effects.

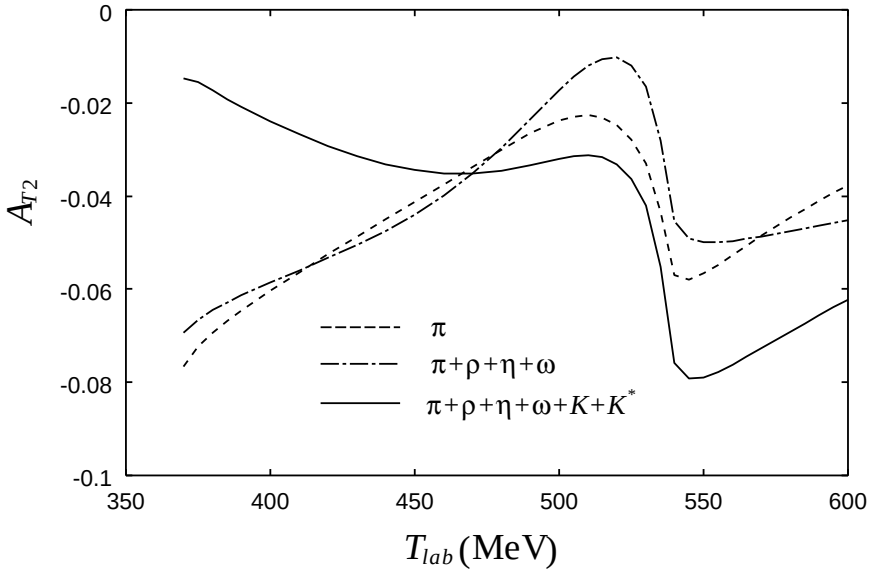

Figure 27: A_{T2}. Solid line shows the all meson exchange mechanism, while the dash-dotted line for only non-strangeness ones. The dash line includes pion-exchange mechanism.

4.3.4 Angular distribution of polarization observables

Angular distribution of polarization observables are presented at 380MeV and 535MeV of incident proton kinetic energies which are two maxima of the total cross section.

At proton energy of 380MeV, which is close to Λ-production threshold, the momentum of final $p\Lambda$ system is about 70MeV/c and we already know the S-wave final states dominates. The differential cross section are shown in Fig. 28. Here we include all the meson exchange mechanism. Solid line includes total angular momentum up to 6. The S and P-wave final states are obviously sufficient at this low energy region. Slight P-wave effect is seen on the differential cross section. Similarly the angular distribution of asymmetry parameters for single polarization $A_{pi}, A_{\Lambda i}$ and double polarization K_{ij} are shown in Figs. 29 and 30 respectively. The angular distribution is similarly dominated by S- and P-wave final states. If we integrate over angle of final states, interference between S and P waves vanishes. Then, as we seen in the previous section, S-wave final state is sufficient. Only the z-component, i.e. the direction of incident proton momentum, of $P_{\Lambda i}, P_{pi}K_{ij}$ are interesting.

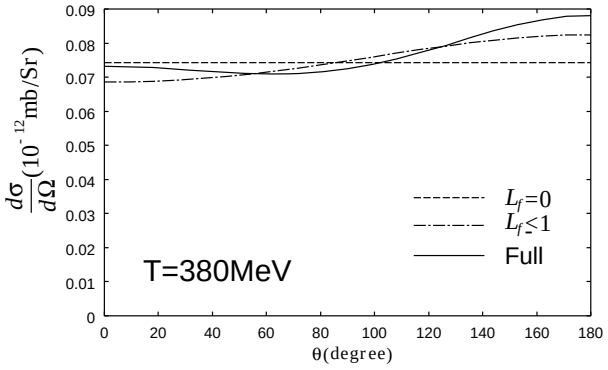

Figure 28: Differential cross section of $p + n \rightarrow p + \Lambda$ at incident proton kinetic energy T=380MeV

At the threshold energy of Σ production, however, D-wave final ΛN state plays dominant role. The differential cross section is given in Fig. 31. The dotted line shows the contributions of final ΛN states up to $L_f \leq 1$, dashed line, $L_f \leq 2$ and solid line $L_f \leq 6$ are summed up.

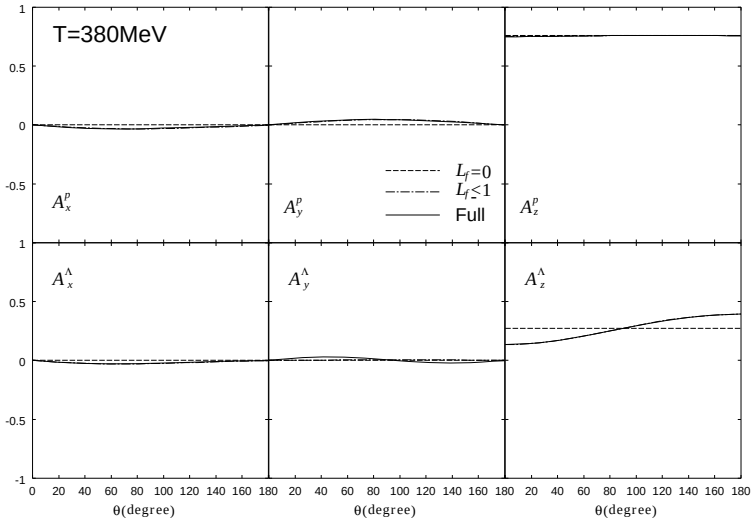

Figure 29: $\vec{A}^p$ and $\vec{A}^\Lambda$ at incident proton kinetic energy T=380MeV

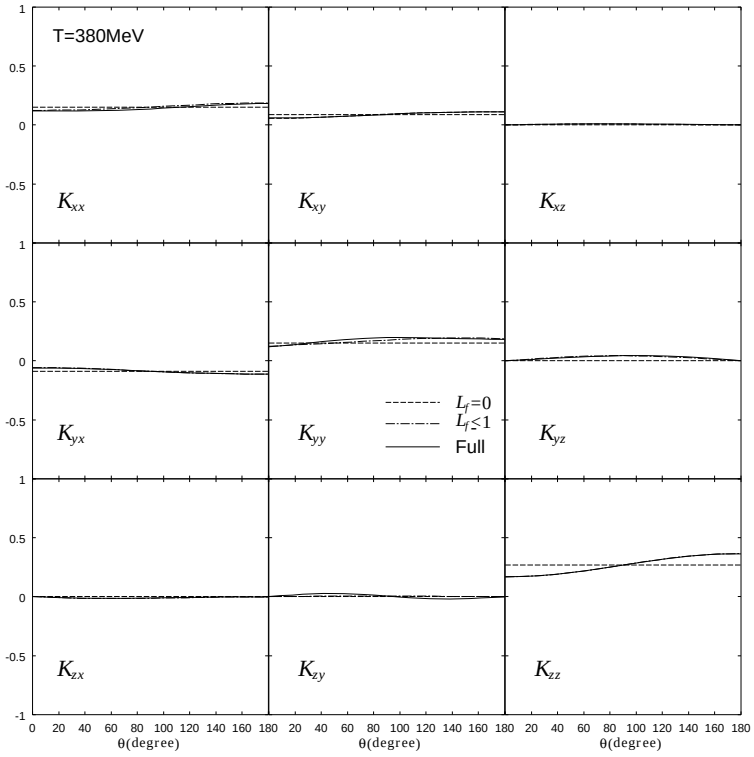

Figure 30: K_{ij} at incident proton kinetic energy T=380MeV

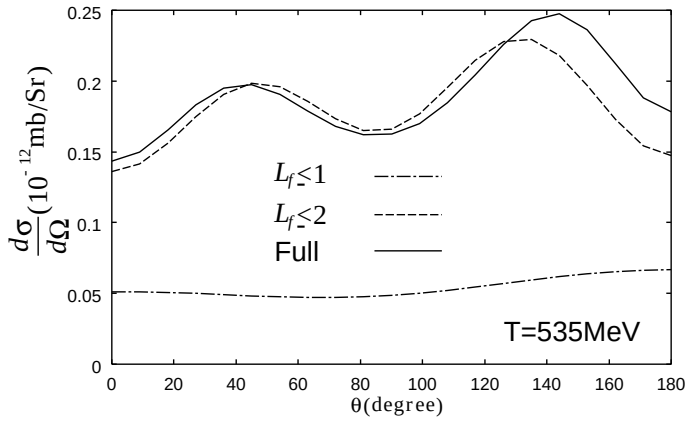

Figure 31: Differential cross section at incident proton kinetic energy T=535MeV

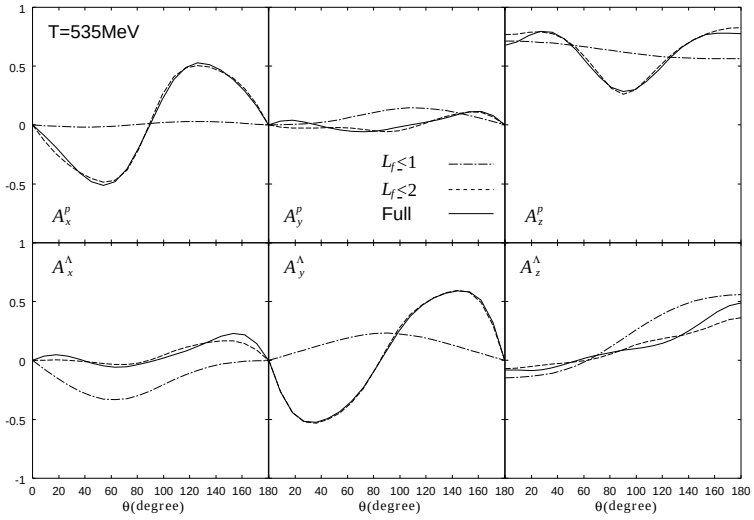

Figure 32: $\vec{A}^p$ and $\vec{A}^\Lambda$ at incident proton kinetic energy T=535MeV

The angular distributions of asymmetry parameter for single and double polarization are shown

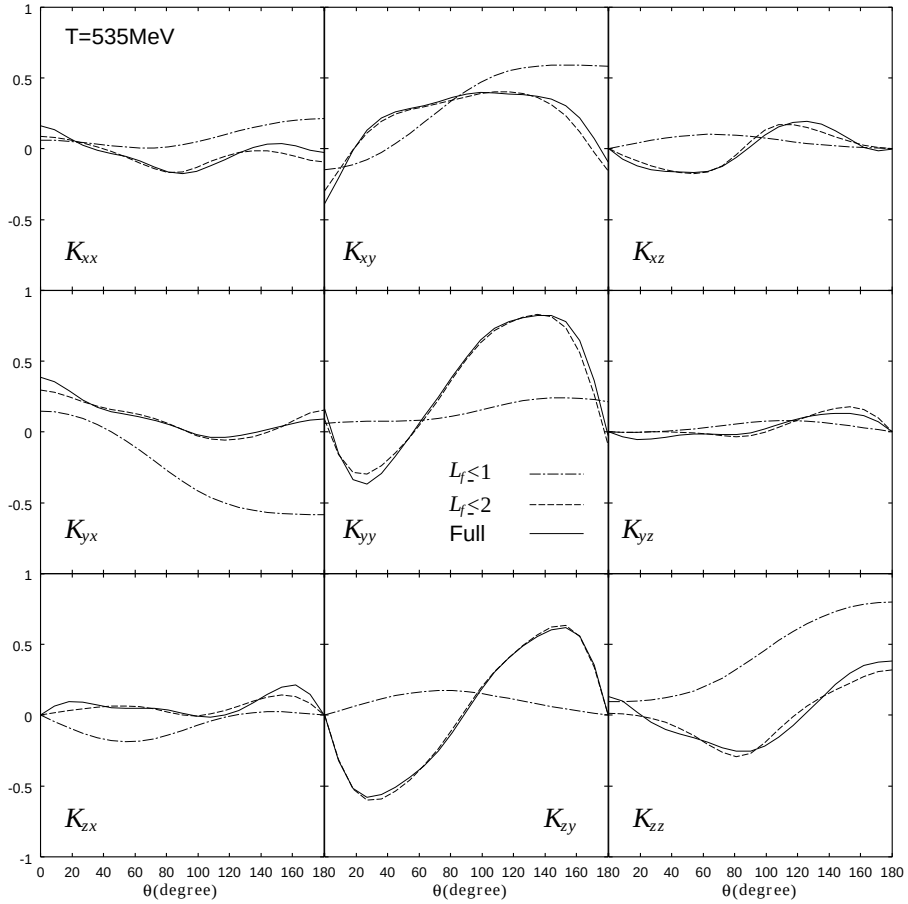

Figure 33: K_{ij} at incident proton kinetic energy T=535MeV

in Figs. 32 and 33, respectively.

In summary, at the low energy region, the reaction is governed by almost the S-wave, and effects of higher partial waves are very small, and angular distribution may not give us additional information unless they are measured with high accuracy. However, at 535MeV, angular distribution will give us definite conclusion on the contributions of higher partial waves.

5 Summary

We have demonstrated the $p + n \to p + \Lambda$ reaction is very useful tool to study the strangeness changing the weak BB interaction. Strong model dependence of polarization observables is useful to clarify the structure of the weak BB interaction.

We have derived general formula of polarization observables with polarized proton beam and the polarization of Λ. At threshold energy of Λ production, we have five independent observables. Four of them are invariant under time reversal. They are measured with single polarization experiment of proton and Λ, which are parity violating quantities. We obtain two additional asymmetries by measuring the double polarization with longitudinal and transverse polarizations. $\bar{A}_\Lambda$ is given by the interference term of the $T = 0$ and 1 NN states, which correspond to the asymmetry parameter α_p of non-mesic decay of hypernuclei. $\bar{A}_p$ measures the interference term of spin triplet and singlet NN states.

We have used meson exchange model of the weak BB interaction, and studied the model dependence of polarization observables. The mechanism of polarization in $p + n \to p + \Lambda$ reaction was rather simply understood by taking into account short range correlation in plane wave approximation. Our numerical results can be summarized as

- Magnitude of the calculated total cross section is the order of 10^{-12}mb, so that the measurement of $p + n \to p + \Lambda$ reaction could be feasible according to Refs. [45, 46].
- Asymmetry parameter of proton, $\bar{A}_p$, is larger than that of Λ, $\bar{A}_\Lambda$. They are both positive.
- The large model dependence of $\bar{A}_p$ will help us to understand the structure of weak BB interaction.
- One of the longitudinal double polarizations, which we denoted as $\bar{A}_{L4}$, is a very interesting observable. It is very sensitive to the D-wave component or strangeness-exchange part of weak transition potential.
- To determine a relative ratio of PV and PC terms, the time reversal invariant transverse double polarization $\bar{A}_{T1}$ is very useful, since the PV and PC amplitudes contribute to

$\bar{A}_{T1}$ with opposite sign.

- We can in principle test time reversal invariance by measuring $\boldsymbol{J}_\Lambda \times \boldsymbol{J}_p \cdot \hat{\boldsymbol{p}}$, which however the trivial initial state and final state interaction gives about 10% polarization.

In conclusion, we found the $p + n \to p + \Lambda$ reaction gives us new informations on weak BB interaction which are different from those of weak non-mesic decay of hypernuclei. The $p + n \to p + \Lambda$ reaction will open a new road to study weak BB interaction.

Acknowledgment

The author would like to express his sincere gratitude to Professor T. Sato for leading the author to finish this work.

He is also indebted to Professor T. -S. H. Lee and Professor V. G. J. Stoks for useful discussions and providing us the YN wave functions.

He also acknowledge Professor T. Kishimoto for his valuable comments and collaboration.

His thanks are also to Mr. H. Nabetani for his kind help in checking this thesis and the members of the Nuclear Theory Group of Osaka University for their useful discussions.

Numerical calculation in this work was carried out at the Information Processing Center at the Fukui Medical University and at Research Center for Nuclear Physics (RCNP), Osaka University.

References

[1] R. Machleidt. Adv. in Nucl. Phys., **19** (1989) 189.

[2] V. G. J. Stoks et al. Phys. Rev, **C49** (1994) 2950.

[3] M. Oka and K. Yazaki. *Quarks and Nuclei*, ed. W. Weise, (World Sci., Singapore) (1984) 489.

[4] R. B. Wiringa, V. G. J. Stoks, and R. Schiavilla. Phys. Rev., **C51** (1995) 38.

[5] P. M. M. Maessen, T. A. Rijken, and J. J. de Swart. Phys. Rev., **C40** (1989) 2226.

[6] T. A. Rijken, V. G. J. Stoks, and Y. Yamamoto. Phys. Rev., **C59** (1999) 21.

[7] B. Holzenkamp, K.Holinde, and J. Speth. Nucl. Phys., **A500** (1989) 485.

[8] A. Reuber, K. Holinde, and J. Speth. Nucl. Phys., **A570** (1994) 543.

[9] K. Tominaga and et al. Nucl. Phys., **A642** (1998) 483.

[10] T. Fujita, Y. Fujiwara, C. Nakamoto, and Y. Suzuki. Prog. Theor. Phys., **100** (1998) 931.

[11] K. Miyagawa and W. Glöckle. Phys. Rev., **C48** (1993) 2576.

[12] K. Miyagawa, H. Kamada, W. Glöckle, and V. Stoks. Phys. Rev., **C51** (1995) 2905.

[13] B. R. Holstein. *Weak Interactions in Nuclei*, (Princeton University Press), 1989.

[14] W. Cheston and H. Primakoff. Phys. Rev., **92** (1953) 1537.

[15] J. J. Szymanski et al. Phys. Rev., **C43** (1991) 849.

[16] H. Noumi et al. Phys. Rev., **C52** (1995) 2936.

[17] S. Ajimura et al. Phys. Lett., **B282** (1992) 293.

[18] S. Ajimura et al. Phys. Rev. Lett., **80** (1998) 3471.

[19] R. H. Dalitz and G. Rajasekharan. Phys. Lett., **1** (1962) 58.

[20] M. M. Block and R. H. Dalitz. Phys. Rev. Lett., **11** (1963) 96.

[21] B. Quinn et al. *Proc. of the IV Int. Symp. on Weak and Electromagnetic Interactions in Nuclei*, ed. H. Ejiri, T. Kishimoto and T. Sato (World Sci., Singapore) (1995) 522.

[22] J. Cohen. Prog. Part. Nucl. Phys., **25** (1990) 139.

[23] E. Oset and A. Ramos. nucl-th/9807018.

[24] M. Ruderman and R. Karplus. Phys. Rev., **102** (1956) 247.

[25] J. B. Adams. Phys. Lett., **22** (1966) 463.

[26] J. B. Adams. Phys. Rev., **156** (1967) 1611.

[27] A. Parreño, A. Ramos, and E. Oset. Phys. Rev., **C51** (1995) 2477.

[28] B. H. J. McKellar and B. F. Gibson. Phys. Rev., **C30** (1984) 322.

[29] G. Nardulli. Phys. Rev., **C38** (1988) 832.

[30] J. F. Dubach. Nucl. Phys., **A450** (1986) 71c.

[31] B. Desplanques, J. F. Donoghue, and B. R. Holstein. Ann. Phys.(N.Y.), **124** (1980) 449.

[32] J. F. Dubach et al. Ann. Phys.(N.Y.), **249** (1996) 146.

[33] A. Parreño, A. Ramos, and C. Bennhold. Phys. Rev., **C56** (1997) 339.

[34] K. Itonaga, T. Ueda, and T. Motoba. Nucl. Phys., **A585** (1995) 331c.

[35] W. M. Alberico, A. De Pace, M. Ericson, and A. Molinari. Phys. Lett., **B256** (1991) 134.

[36] A. Ramos, M. J. Vicente-Vacas, and E. Oset. Phys. Rev., **C55** (1997) 735.

[37] E. Oset and L. L. Salcedo. Nucl. Phys., **A443** (1985) 704.

[38] C. -Y. Cheung, D. P. Heddle, and L. S. Kisslinger. Phys. Rev., **C27** (1983) 335.

[39] D. P. Heddle and L. S. Kisslinger. Phys. Rev., **C33** (1986) 608.

[40] T. Inoue, S. Takeuchi, and M. Oka. Nucl. Phys., **A597** (1996) 563.

[41] T. Inoue, M. Oka, T. Motoba, and K. Itonaga. Nucl. Phys., **A633** (1998) 312.

[42] M. Oka. Nucl. Phys., **A639** (1998) 317c.

[43] H. Nifenecker. Z. Phys., **A346** (1993) 171.

[44] T. Kishimoto. *Proc. of the IV Int. Symp. on Weak and Electromagnetic Interactions in Nuclei*, ed. H. Ejiri, T. Kishimoto and T. Sato (World Sci., Singapore) (1995) 514.

[45] T. Kishimoto. Nucl. Phys., **A629** (1998) 369c.

[46] T. Kishimoto et al. RCNP proposal, E122.

[47] N. Panchapakesan. Ann. Phys.(N.Y.), **45** (1967) 172.

[48] D. S. Beder. Nucl. Phys., **B49** (1972) 45.

[49] J. Haidenbauer et al. Phys. Rev., **C52** (1995) 3496.

[50] A. Parreño, A. Ramos, N. G. Kelkar, and C. Bennhold. nucl-th/9810020.

[51] H. Nabetani, T. Ogaito, T. Sato, and T. Kishimoto. nucl-th/9812072.

[52] H. Bandō, T. Motoba, and J. Žofka. Int. J. Mod. Phys., **A5** (1990) 4021.

[53] B. H. J. McKellar and P. Pick. Phys. Rev., **D7** (1973) 260.

Appendix A

In this appendix we summarize the functions $\mathcal{Y}$ and $\mathcal{Z}$ which appeared in the formula of the polarization asymmetries.

$$\mathcal{Y}^1_{LL'}(x) = \delta_{L,L'+1}\left[(-)^{L'}\sqrt{\frac{3}{L'+1}}P'_{L'+1}(x)\right] + \delta_{L,L'-1}\left[(-)^{L'}\sqrt{\frac{3}{L'}}P'_{L'-1}(x)\right] \quad (A.1)$$

$$\mathcal{Y}^2_{LL'}(x) = \delta_{L,L'+1}\left[(-)^{L'+1}\sqrt{\frac{3}{L'+1}}P'_{L'}(x)\right] + \delta_{L,L'-1}\left[(-)^{L'+1}\sqrt{\frac{3}{L'}}P'_{L'}(x)\right] \quad (A.2)$$

$$\mathcal{Y}^3_{LL'}(x) = \delta_{L,L'}\, i(-)^{L+1}\sqrt{\frac{3[L]}{L(L+1)}}P'_L(x) \quad (A.3)$$

$$\mathcal{Z}^1_{LL'}(x) = -\frac{1}{3\sqrt{5}}(W^1_{LL'} + W^2_{LL'} + xW^3_{LL'}) \quad (A.4)$$

$$\mathcal{Z}^2_{LL'}(x) = \frac{1}{\sqrt{5}}W^1_{LL'} \quad (A.5)$$

$$\mathcal{Z}^3_{LL'}(x) = \frac{1}{\sqrt{5}}W^2_{LL'} \quad (A.6)$$

$$\mathcal{Z}^4_{LL'}(x) = \frac{1}{2\sqrt{5}}W^3_{LL'} \quad (A.7)$$

$$\mathcal{Z}^5_{LL'}(x) = \frac{i}{2\sqrt{10}}W^4_{LL'} \quad (A.8)$$

$$\mathcal{Z}^6_{LL'}(x) = \frac{i}{2\sqrt{10}}W^5_{LL'} \quad (A.9)$$

$$W^1_{LL'} = [\delta_{L,L'+2}\bar{x}(1,L') + \delta_{L,L'}\bar{x}(2,L) + \delta_{L,L'-2}\bar{x}(1,L)]P''_L(x) \quad (A.10)$$

$$W^2_{LL'} = [\delta_{L,L'+2}\bar{x}(1,L') + \delta_{L,L'}\bar{x}(2,L) + \delta_{L,L'-2}\bar{x}(1,L)]P''_{L'}(x) \quad (A.11)$$

$$W^3_{LL'} = -2\delta_{L,L'+2}\bar{x}(1,L')P''_{L'+1} - \delta_{L,L'}\bar{x}(2,L)(P'_{L'}(x) + 2xP''_{L'}(x)) - 2\delta_{L,L'-2}\bar{x}(1,L)P''_{L'-1}(x) \quad (A.12)$$

$$W^4_{LL'} = [\delta_{L,L'+1}\bar{x}(3,L') - \delta_{L,L'-1}\bar{x}(3,L)]P''_L(x) \quad (A.13)$$

$$W^5_{LL'} = [-\delta_{L,L'+1}\bar{x}(3,L') + \delta_{L,L'-1}\bar{x}(3,L)]P''_{L'}(x) \quad (A.14)$$

$$\bar{x}(1,L) = (-)^L\sqrt{\frac{5}{(L+1)(L+2)(2L+3)}} \quad (A.15)$$

$$\bar{x}(2,L) = (-)^L \sqrt{\frac{30[L]}{L(L+1)(2L-1)(2L+3)}} \tag{A.16}$$

$$\bar{x}(3,L) = (-)^{L+1} \sqrt{\frac{20}{L(L+1)(L+2)}} \tag{A.17}$$